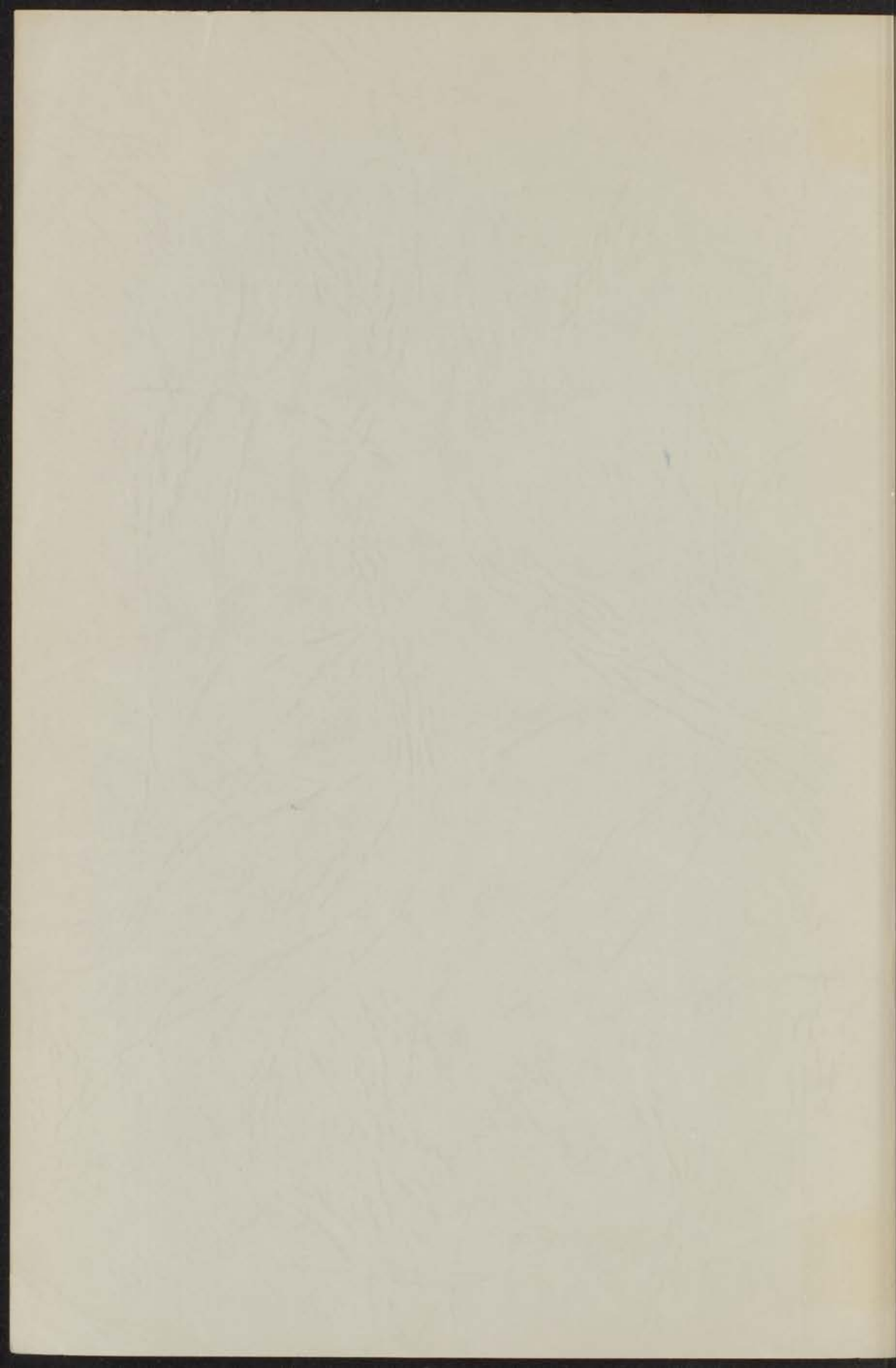# THE INFLUENCE OF A MAGNETIC FIELD ON THE TRANSPORT PROPERTIES OF GASES OF POLYATOMIC MOLECULES

J. KORVING

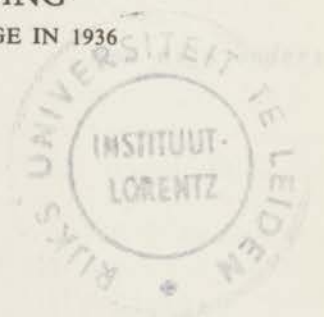# THE INFLUENCE OF A MAGNETIC FIELD ON THE TRANSPORT PROPERTIES OF GASES OF POLYATOMIC MOLECULES

DOOR

JOHANNES KORVING

GEBOREN TE 'S-GRAVENHAGE IN 1936

Promotor: Prof.Dr.   J.J.M. Beenakker

Aan mijn ouders

STELLINGEN

I. Op grond van symmetrie beschouwingen kan worden aangetoond
    dat in een magnetisch veld transversale effecten in diffusie,
    warmtegeleiding en thermodiffusie enerzijds en in viscosi-
    teit anderzijds mogelijk zijn, maar dat kruiseffecten tussen
    beide groepen verschijnselen niet bestaan. In een electrisch
    veld daarentegen, bestaat de mogelijkheid tot impulstrans-
    port t. g. v. een gradiënt in de temperatuur of in de concen-
    tratie en evenzo, energie- en deeltjestransport t. g. v. een
    snelheidsgradiënt.

> c.f. S.R. de Groot and P. Mazur, Non-equili-
> brium thermodynamics, (North-Holland Publish-
> ing Cy., Amsterdam, 1962).

II. Voor het aantonen van de invloed van een magnetisch veld op
    de transport-verschijnselen in gassen, biedt een onderzoek
    naar het optreden van transversaal transport voordelen boven
    een onderzoek naar de verandering van de normale transport-
    coëfficiënten.

III. De richting van het electrisch dipoolmoment in CO is C^-O^+.

IV. Het door Choy en Raw geconstateerde verschil tussen de uit
    experimentele grootheden bepaalde Eucken-factor voor CF_4
    en de waarde die volgt uit berekeningen voor het "rough
    sphere model", is eenvoudig te verklaren.

> P. Choy and C.J.G. Raw, J.chem.Phys. 45 (1966)
> 1413.

V. Senftleben heeft experimenten verricht betreffende de veran-
    dering van het warmtegeleidingsvermogen van gassen onder in-
    vloed van een electrisch veld. De presentatie van de experi-
    mentele resultaten is gebaseerd op een onjuiste interpreta-
    tie.

> H. Senftleben, Ann. Phys. 15 (1965) 273.

VI. Het opgeven van de equivalente ruisspanning aan de ingang van een electronisch instrument, geeft onvoldoende informatie over de gevoeligheid.

VII. De wijze waarop Walker en Westenberg uit hun diffusie experimenten de waarde van de exponent van de afstotende potentiaal voor de He-Ar wisselwerking afleiden, is niet correct.

R.E. Walker and A.A. Westenberg, J.chem.Phys. 31 (1959) 519.

VIII. Het is te verwachten dat de verandering van de viscositeit en de warmtegeleiding onder invloed van een magnetisch veld voor gassen met een totale kernspin verschillend van nul, bij zeer lage drukken niet zal bestaan.

IX. Jobst gaat bij zijn metingen van de warmtegeleiding van gassen volgens de niet-stationaire draadmethode, voorbij aan de uitzetting van het gas bij verwarming. Hierdoor moet minstens getwijfeld worden aan de betrouwbaarheid van zijn resultaten.

W. Jobst, diss. Zürich (1964).

CONTENTS

CHAPTER I

VISCOSITY

1.1 Introduction

In 1930 S e n f t l e b e n[1] discovered that the thermal conduc-
tivity of gaseous O_2 is influenced by a magnetic field. Further
studies[2] showed that viscosity was also affected. The fact that
under the influence of the magnetic field NO behaved in the same
way as O_2, suggested that this phenomenon - known now by the name
of its discoverer - was a property of paramagnetic gases. The
Senftleben-effect was extensively studied for nearly a decade[3-12].
The results of this work may be summarized in the following way.
In the presence of a magnetic field, H, the transport coefficients
of a paramagnetic gas decrease slightly. The effect is an even
function of H and saturates at high values of H. At constant
temperature the approach to saturation is a unique function of
H/p, where p is the pressure. In mixtures with a non-paramagnetic
gas the change of the transport coefficients is proportional to
the concentration of the paramagnetic component.

This results led G o r t e r[13] to a qualitative interpretation
based on a change in the mean free path of an O_2 molecule caused
by the magnetic field. This idea was later elaborated more
quantitatively by Z e r n i k e and V a n L i e r[14]. They
assumed, following G o r t e r, that a fast rotating, paramagne-
tic, diatomic molecule can be imagined as a disc with a magnetic
moment, μ, in the direction of the axis of rotation. The collision
cross-section of such a molecule depends on the angle between the
velocity and the axis of rotation. Normally the direction of the
axis of rotation is conserved between two collisions. In the pre-
sence of a magnetic field, however, the magnetic moment and there-
fore the axis of rotation that is coupled to it will - in this
classical picture - precess around the field direction with the
Larmor frequency, ω_L. This precession gives rise to a periodic

7

change of the collision cross-section of the molecule. Hence, between two collisions an extra averaging takes place over the non-spherical part of the cross-section resulting in an increase in the collision probability. The changes in the transport properties are thus related to the non-sphericity of the molecule. This leads to a decrease in the viscosity and the thermal conductivity. The number of precessions between two successive collisions determines the extent of that extra averaging. Since the Larmor frequency is proportional to μH and the collision frequency, ω_C, is proportional to p, the approach to saturation can be described as a function of H/p. Saturation takes place when ω_L is sufficiently higher than ω_C. The linear concentration dependence follows also immediately from this picture.

Originally this effect was thought to be limited to paramagnetic gases like O_2 and NO. We showed that this limitation is not real and the influence of a magnetic field on the transport properties is common to nearly all polyatomic molecules[15]. We used the following argument. In general a polyatomic molecule has - be it small - a magnetic moment caused by its rotation. In the picture of G o r t e r, the change in the transport properties at saturation does not depend on the magnetic moment but only on the non-sphericity of the molecule. Hence one may expect that diamagnetic N_2 will also show an effect of the same order of magnitude as paramagnetic O_2 if one is able to obtain a comparably complete averaging during the flight-time between collisions. The smallness of the rotational magnetic moments, however, leads to lower precession frequencies, so higher magnetic fields and lower pressures are required to reach saturation for non-paramagnetic gases.

As this effect has the unique character that it is directly related to the non-spherical part of the molecular interaction - it is absent in the case of noble gases - this phenomenon gives us a new tool in the study of the transport properties of polyatomic molecules. At this moment the state of affairs is such that, whenever theoretical calculations for non-spherical molecules are performed, it is difficult to decide whether the description is really improved over that of simple elastic spherical molecules. This difficulty stems from the fact that in simple polyatomic molecules the transport properties are, apart from trivial effects (e.g. the Eucken factor), only influenced in second order by the non-sphericity. So, all the more refined theory gives is a small

8

contribution to the dominant spherical behaviour. Hence it is clear that it is rather important in the study of non-spherical molecules to find a measurable transport quantity which is mainly determined by the non-sphericity itself.

A good illustration is given by the following example. Recently there has been some discussion on the character of the distribution function of velocities and angular momenta of polyatomic molecules in a non-uniform gas. W a l d m a n n[16-19] and K a - g a n and A f a n a s e v[20] showed that the usual assumption that the distribution function is isotropic in angular momentum is not valid and that one has to include terms that are anisotropic in both velocity, V, and angular momentum, M. Thus a macroscopic gradient gives rise not only to an anisotropy in V but also through the collision mechanism to an anisotropy in M. The magnetic field effects are, as shown by K a g a n and M a k - s i m o v[21], directly related to this anisotropy in M and its coupling with V. Measurements of the field effect give direct information on the contribution of the anisotropy in M[22].

Another example of the possibilities offered by this new experimental method is the information that can be obtained from the field dependence of the effect. From the simple geometric mean free path picture, it is already clear that the field dependence saturates when averaging by the precession between collisions is complete i.e., as soon as the Larmor frequency is much higher than the collision frequency. One might expect that the form of the curve of the effect versus H/p will be a general property of the phenomenon and will give as such only scant information. Knowing the magnetic moment of the molecule, the value of H/p for which half of the saturation is reached, $(H/p)_{\frac{1}{2}}$, gives, however, the characteristic time, τ, that corresponds to the collision process that is disturbed. As soon as the phenomenon is no longer related to a pure geometrical property of the elastic collision cross-section, this time is not necessarily of the order of the time between two successive collisions, but might be the time between two inelastic collisions. The latter can be much higher than the former.

As soon as a reliable theory is available the measurements will also give quantitative information on the molecular magnetic moment and on the non-sphericity of the intermolecular interaction.

From the description in terms of anisotropy in M it is clear that

the influence of a magnetic field on the transport properties is not limited to linear molecules. Any coupling mechanism between v and M will be effective. Hence molecules like CH_4, CD_4 and CF_4 will also show the field effects[23].

Till now we only regarded the change in the transport coefficients η and λ in the presence of a magnetic field as the change of a scalar quantity. Without field the gas can be considered as an isotropic system so that the transport coefficients are indeed scalars. In a field, however, a polyatomic gas becomes anisotropic and the transport coefficients get a tensorial character. This problem has been extensively treated by D e   G r o o t   and M a z u r[24] in their book on non-equilibrium thermodynamics. They show that a magnetic field introduces phenomena similar to the magneto resistance effect in electrical conductivity. Furthermore transverse effects appear i.e., energy and momentum transport perpendicular to gradient and field direction can occur, a phenomenon similar to the Hall-effect.

In the last years we studied the different magnetic effects in several gases. We investigated the change in the viscosity for O_2, NO, N_2, CO, normal H_2, para H_2, normal D_2, ortho D_2, HD, CH_4, CD_4, CF_4 and CO_2. Transverse momentum transport was studied in O_2, N_2 and HD and thermal conductivity experiments were performed on O_2, NO, N_2, CO and CH_4. In this chapter we will report on the experimental results for the viscosity. In chapter II we will give the experimental results obtained for the thermal conductivity. This is followed by a general discussion, including the transverse effect[25], in chapter III, where the emphasis will be on the theoretical aspects of the now available experimental information.

1.2 Experimental method and apparatus

The choice of our apparatus was mainly determined by the smallness of the effect; the magnitude of the change in the viscosity at saturation is about 0.4% for O_2. Therefore an absolute viscosity determination cannot be used because the available techniques do not yield a sufficient accuracy. The obvious solution is a differential method in which only the change of the viscosity is measured. For this purpose we chose a method similar to the one introduced by E n g e l h a r d t   and   S a c k[2] and also used by B e c k e r[26] in his study on the difference between   the

10

viscosities of ortho H_2 and para H_2, i.e., a capillary Wheatstone bridge. The change of the viscosity caused by a magnetic field is then given directly by the unbalance of the bridge. As a consequence of the desired high H/p values the absolute pressure and thus also the pressure difference over the bridge $(p_A - p_B)$ is rather low (5 - 10 mm Hg). For this reason the unbalance of the bridge when the field is switched on is very small (10^{-3} - 10^{-4} mm Hg). Hence a capacitive differential manometer with high sensitivity (10^{-5} mm Hg) was used (Atlas Membran Mikro Manometer). Since pressure fluctuations across the bridge are mainly caused by temperature fluctuations of the capillaries and as a small temperature drift is unimportant, we surrounded the bridge by a non-circulating waterbath in a cryostat. To further attenuate the temperature variations the capillaries are thermally insulated from direct contact with the bath. In this way a short range temperature stability of the capillary bridge of better than 10^{-3} °C was attained. Furthermore, the output of the manometer is fed into a recorder. In this manner the remaining small pressure fluctuations can easily be averaged out, giving a further increase in resolution. Under these conditions we are able to detect relative viscosity changes of 2.10^{-6}.
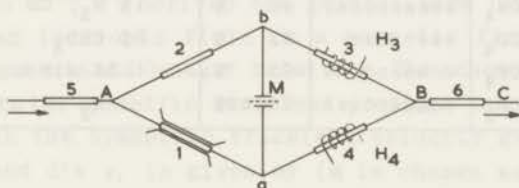
Fig. 1.1

A schematic diagram of the apparatus.

A scheme of the apparatus is drawn in fig. *1.1*. The capillaries C_1, C_2, C_3 and C_4 are chosen equal. In most cases we used capillaries with 0.8 mm diameter and 40 mm length. Complete balancing can be attained by heating either C_3 or C_4 by means of the heaters H_3 and H_4 respectively. In this way the effective flow resistance of the capillary is varied by changing the viscosity and the density of the gas. The pressure in the bridge can be regulated by means of the capillaries C_5 and C_6; C_5 is

11

connected to the gas supply and C_6 is leading to a vacuum pump.
The capillary C_1 is placed between the poles of a magnet with the
field direction perpendicular to the flow direction. When the
field is switched on the viscosity in C_1 decreases, resulting in
a rise in pressure at "a". The pressure difference between "a"
and "b" is immediately related to the change in the flow resistance
of C_1.

In table 1.I the origin and purity of the gases studied are given.

Table 1.I

gas	origin	purity	main impurities if known
O_2	commercial	99.95%	
NO	commercial	99 %	0.4% CO_2
N_2	commercial	99.95%	
CO	commercial	98 %	0.5% N_2
H_2	commercial	99.95%	
D_2	see text	99.7 %	HD
HD	see sext	99.7 %	D_2
CH_4	commercial	98 %	1% N_2, CO
CD_4	see text	92 %	8% CHD_3
CF_4	commercial	95 %	1.5% air
CO_2	commercial	99.85%	N_2

D_2 was prepared by electrolysis of D_2O and HD was formed by the
chemical reaction:

$$Li\ Al\ H_4 + 4\ D_2O \longrightarrow Li\ OD + Al\ (OD)_3 + 4\ HD.$$
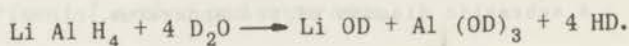
Small amounts of HD in D_2 or H_2 and D_2 in HD were extracted in a
rectification column[27] so that a purity better than 99.7% was
attained, as was demonstrated in a thermal diffusion experiment.
Para H_2 and ortho D_2 were prepared by condensing normal H_2 or
normal D_2 on a catalyst at $20°K$.

Comparatively large amounts of CD_4 were obtained making use of
the exothermic chemical equilibrium:

$$CO + 3\ D_2 \rightleftharpoons CD_4 + D_2O \quad [28]$$

12
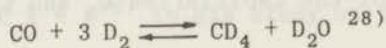
This was done by leading a mixture containing 95% D_2 and 5% CO over a CrNi catalyst at 300°C. Under these conditions nearly all CO reacted. In this way CD_4 with about 8% CHD_3 was obtained as was shown by a mass-spectrometer analysis*. Measurements with various concentrations of CHD_3 (8 - 30%) exhibited only a small dependence on the CHD_3 concentration.

1.3 Calculation of the results

It was often tacitly assumed (see e.g. ref. 2) that in an ideal bridge circuit the relative change in η caused by a magnetic field is still given by the expression derived from Poiseuille's law, i.e.,

$$- \frac{\Delta \eta}{\eta_o} = 4 \frac{p_a - p_b}{p_A - p_B} \tag{1.1}$$

We will discuss here how far this is correct. As was already pointed out in the introduction the magnetic field changes the character of the viscosity. H o o y m a n , M a z u r and D e G r o o t[24, 29] derived the general form for the viscosity tensor of an isotropic fluid in a magnetic field using space symmetry arguments and Onsager relations. The scheme of coefficients that connects the symmetric traceless pressure tensor, $\overset{o\,s}{\Pi}$, and the trace Π with the symmetric traceless velocity gradient tensor, $(\overset{o}{\text{Grad}}\ v)^s$, and div v, is given by (H is chosen as the x-axis)

	$(\overset{o}{\text{Grad}}\ v)^s_{xx}$	$(\overset{o}{\text{Grad}}\ v)^s_{yy}$	$(\overset{o}{\text{Grad}}\ v)^s_{zz}$	$(\overset{o}{\text{Grad}}\ v)^s_{yz}$	$(\overset{o}{\text{Grad}}\ v)^s_{zx}$	$(\overset{o}{\text{Grad}}\ v)^s_{xy}$	div v
$\overset{o\,s}{\Pi}_{xx}$	$-2\eta_1$	0	0	0	0	0	-2ζ
$\overset{o\,s}{\Pi}_{yy}$	0	$-2\eta_2$	$-2(\eta_1-\eta_2)$	$-2\eta_4$	0	0	ζ
$\overset{o\,s}{\Pi}_{zz}$	0	$-2(\eta_1-\eta_2)$	$-2\eta_2$	$2\eta_4$	0	0	ζ
$\overset{o\,s}{\Pi}_{yz}$	0	η_4	$-\eta_4$	$-2(2\eta_2-\eta_1)$	0	0	0
$\overset{o\,s}{\Pi}_{zx}$	0	0	0	0	$-2\eta_3$	$-2\eta_5$	0
$\overset{o\,s}{\Pi}_{xy}$	0	0	0	0	$2\eta_5$	$-2\eta_3$	0
Π	-2ζ	ζ	ζ	0	0	0	$-\eta_v$

$$\tag{1.2}$$

* W e t h a n k Dr. A.E. de Vries of the Laboratorium voor Atoom- en Molecuulfysica (Amsterdam) for analysing CD_4.

13

The elements of this scheme are even in H except for η_4 and η_5 which are odd. In the field free case $\eta_1=\eta_2=\eta_3=\eta_0$ and $\eta_4=0$, $\eta_5=0$, $\zeta=0$. In the approximation of the flow of an incompressible fluid, the part of the scheme which is relevant for our measurements, is encircled. As we know now from our work on the transverse effect[25] the off-diagonal element (η_5) is of the same order of magnitude as the change in the diagonal elements $(2\eta_2 - \eta_1$ and $\eta_3)$. Hence one has to consider also a possible influence of η_5 on the flow resistance.

For this purpose one has to solve the Navier-Stokes equations for the anisotropic case. One obtains for an incompressible fluid with $\partial v_x/\partial x = 0$ and $\partial v_y/\partial y = 0$

$$\rho \frac{d\mathbf{v}}{dt} = -\nabla p - \nabla.\overset{o\,s}{\Pi} \tag{1.3}$$

where ρ is the density and $\mathbf{v}$ the flow velocity; $\overset{o\,s}{\Pi}$ can be expressed in the corresponding velocity gradients by means of the scheme (1.2) of H o o y m a n, M a z u r and D e G r o o t[29].

Fortunately, the problem is simplified as a result of the cylindrical symmetry of the set up. In this situation, with the field
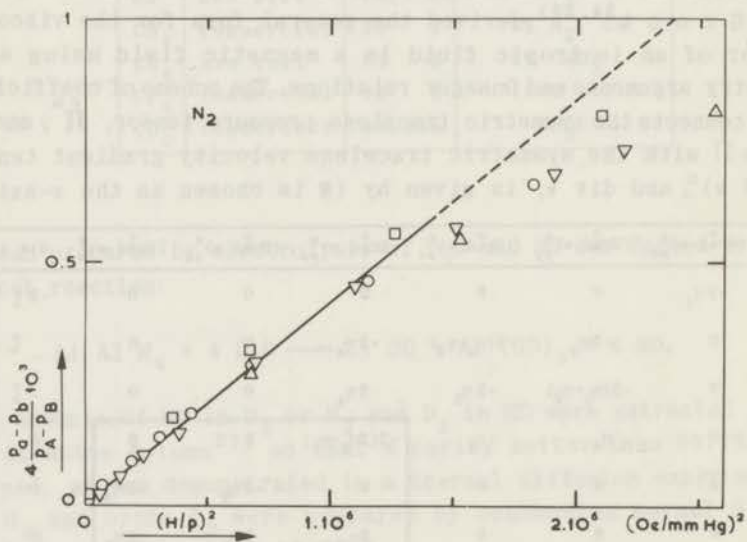
Fig. 1.2

$4(p_a - p_b)/(p_A - p_B)$ as a function of $(H/p)^2$ for N_2.

14

perpendicular to the capillary, the flow resistance has to be an even function of the field. Together with eq. *(1.3)* this means that the off-diagonal elements, which are odd in H can contribute only in the order $(\eta_5/\eta_0)^2$. Indeed no lower powers than $(H/p)^2$ have been found as is illustrated in fig. *1.2* where for N_2, $4(p_a-p_b)/(p_A-p_B)$ is plotted versus $(H/p)^2$. Neglecting the contribution of η_5, the solution of equation *(1.3)* for an incompressible fluid is of the well known Poiseuille type

$$v_x = 0$$
$$v_y = 0$$
$$v_z = -\frac{R^2 - x^2 - y^2}{2(2\eta_2 - \eta_1 + \eta_3)}\frac{\partial p}{\partial z} \qquad (1.4)$$

so for an ideal bridge circuit expression *(1.1)* is indeed valid

with

$$\Delta\eta = \frac{1}{2}(2\eta_2 - \eta_1 + \eta_3 - 2\eta_0) \qquad (1.5)$$

The solution *(1.4)* does not change essentially in going over to compressible gas flow. Already in the field free case the friction losses arising from the appearance of $\partial^2 v_z/\partial z^2$ are negligible.

A disadvantage of our set up is that we determine the average of $(2\eta_2 - \eta_1)$ and η_3, and not the coefficients separately. Although

Fig. 1.3
A schematic diagram of the set-up for the determination of η_3 (*a*) and $2\eta_2-\eta_1$ (*b*) in a slit arrangement.

15

a slit arrangement allows a direct determination of $(2\eta_2 - \eta_1)$ and η_3 (see figs. *1.3a* and *1.3b*) we decided to measure in a capillary for two reasons. First of all the cross-section of slit arrangements is generally bigger than for capillaries, in order to avoid end effects $(d \ll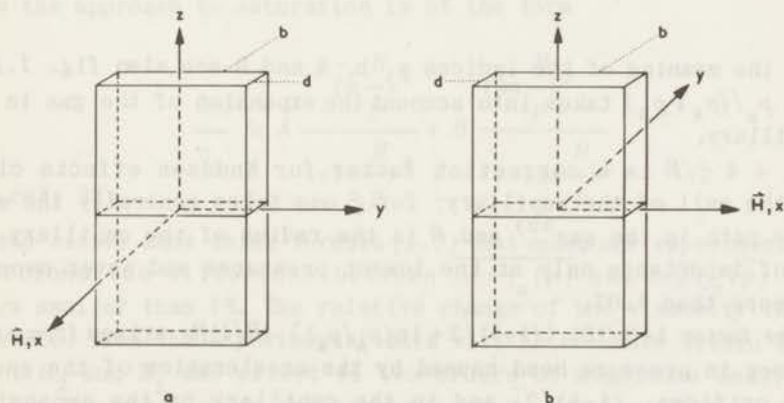 b)$. Since for equal cross-section the slit width, d, is appreciably smaller than the diameter of a corresponding capillary, Knudsen effects will occur already at much higher pressures. Furthermore a slit arrangement requires a much larger field space than a comparable capillary set-up. Thus for two reasons this would severely limit the available H/p range. Using a capillary had the advantage that we could compare our results for O_2 and NO directly with the experiments of S e n f t l e b e n e.a.. Naturally one can measure η_3 with the field parallel to the capillary. Till now this was not possible since the required high magnetic field was not available in such an arrangement.

Because the flow in the bridge circuit is not ideal Poiseuille type, one has

$$-\frac{\Delta\eta}{\eta_o} = f \, 4 \, \frac{p_a - p_b}{p_A - p_B}$$

with (1.6)

$$f = \frac{2p_a}{p_A + p_B} \, (1 + 4\frac{\xi}{R}) \, \{1 + \frac{1}{16} \, (\frac{1+k}{2} + \ln\frac{p_A}{p_a}) \, \frac{R}{l} Re\}$$

For the meaning of the indices a, b, A and B see also fig. *1.1*.

$2 \, p_a/(p_A + p_B)$ takes into account the expansion of the gas in the capillary.

$1 + 4 \, \xi/R$ is a correction factor for Knudsen effects close to the wall of the capillary; for ξ one takes generally the mean free path in the gas[30] and R is the radius of the capillary. It is of importance only at the lowest pressures and never amounts to more than 1.07.

The factor $1 + (1/16) \, \{(1+k)/2 + \ln(p_A/p_a)\} \, (R/l) Re$ arises from extra losses in pressure head caused by the acceleration of the gas at the orifices, $(1+k)/2$, and in the capillary by the expansion: $\ln(p_A/p_a)$. l is the length of the capillary, k a constant depending on the shape of the entrance (k varies between 0 and 1) and Re Reynolds number. This factor was nearly always unity.

Expression *(1.6)* is derived from the general formula for Hagen-Poiseuille flow:

$$\frac{p_A^2 - p_a^2}{2} \left(1 + 4\frac{\xi}{R}\right) = \frac{8\eta_0 l}{\pi R^4} \frac{G}{\rho_0} \left\{1 + \frac{1}{16}\left(\frac{1+k}{2} + \ln\frac{p_A}{p_a}\right)\frac{R}{l} Re\right\} \qquad (1.7)$$

(see also ref. 31)

Here G is the total mass transport per unit time. $\rho_0 = M/RT$ with M the molecular weight, R the gasconstant and T the absolute temperature.

A correction for the stray field of the magnet was only applied for the lowest pressures of O_2 and NO and could be neglected completely for measurements of the other gases. The bridge was checked with He gas which exhibited no effect when the field was switched on, as was to be expected.

Since $\Delta\eta/\eta_0$ is a function of H/p and p varies over the length of the capillary we measure in fact an average given by the expression:

$$\overline{\frac{\Delta\eta}{\eta_0}}^l (p) = \frac{1}{l}\int_0^l \frac{\Delta\eta}{\eta_0}(p_z)\, dz$$

Since the approach to saturation is of the form

$$\frac{\Delta\eta}{\eta_0} = A\frac{(a\frac{H}{p})^2}{1 + (a\frac{H}{p})^2} + B\frac{(2a\frac{H}{p})^2}{1 + (2a\frac{H}{p})^2}$$

(see ref. 22).

one can easily show using formula *(1.7)* that under our experimental conditions the difference between $\overline{\Delta\eta/\eta_0(p)}$ and $\Delta\eta/\eta_0(\bar{p})$ is always smaller than 1%. The relative change of the viscosity thus calculated from the experimental data will be accurate within 5%. As for H_2 and D_2 the effect is two orders of magnitude smaller than for the other gases the accuracy for H_2 and D_2 will be mainly determined by the resolution of the apparatus. One expects that their saturation values are accurate within 15% and 10% respectively.

17

1.4 Experimental results and discussion

We will first discuss the rather extensive experiments on O_2, which were performed to check the apparatus and to compare with existing data. As it is important to be able to reach high H/p values the apparatus was especially tested for good performance in the low pressure region. Experiments were carried out at room temperature from 5 mm Hg up to 1 atmosphere and with two different capillary diameters: 0.96 mm and 0.58 mm. The results confirm fully the H/p dependence over the whole pressure range, while no dependence on the capillary diameter was observed (see fig. *1.6*). The available data are those of

a S e n f t l e b e n e.a. whose results are in good agreement with the H/p law at high pressures. This is, however, not the case for pressures below 100 mm Hg.

b S a c k[4], whose measurements over a pressure range between 10 and 760 mm Hg suggest a pressure independent effect.

c M e r c e a and U r s u[32], who found an influence of the diameter of the capillary on the effect.
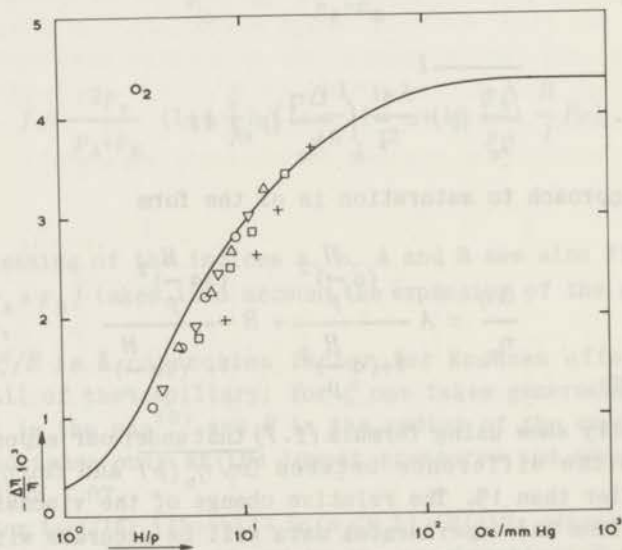
Fig. 1.4

A comparison of our results with the corrected data of S e n f t-
l e b e n and G l a d i s c h for O_2. ———— our results.
S e n f t l e b e n and G l a d i s c h: ○ 650 mm Hg, ▽ 550 mm Hg,
△ 450 mm Hg, □ 350 mm Hg, + 250 mm Hg.

18

We have the impression that part of the discrepancy with older results stems from the fact that these authors did not correct for expansion and slip. This makes also a comparison with existing data for O_2 and NO rather difficult. In one case (measurements on O_2 by S e n f t l e b e n and G l a d i s c h[9]) enough details are available to recalculate the data taking into account the expansion of the gas. The results are then in reasonable agreement with our experiments (see fig. 1.4). In fig. 1.5 our data for NO are compared with those of S e n f t l e b e n and G l a - d i s c h[12].
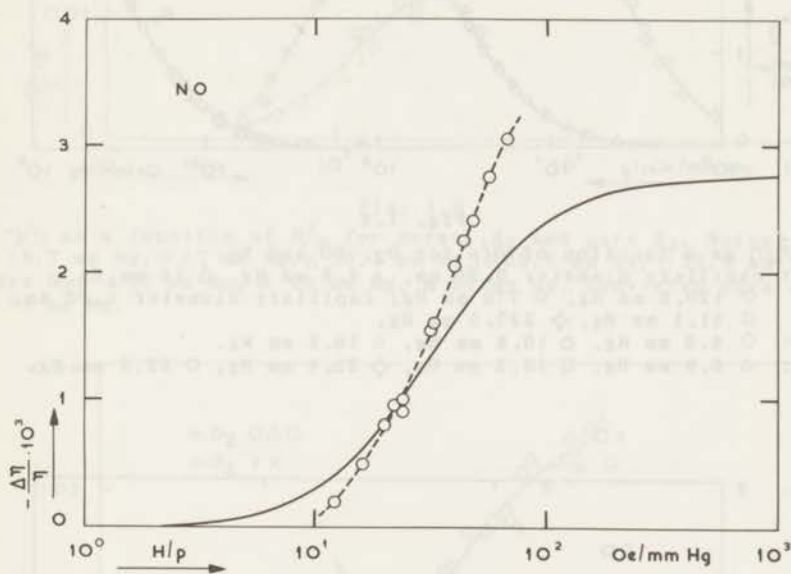
Fig. 1.5

A comparison of our results with the measurements of S e n f t - l e b e n and G l a d i s c h for NO. ——— our results. O S e n f t l e b e n and G l a d i s c h.

A survey of our results is given in figs. 1.6, 1.7, 1.8, 1.9, 1.10, 1.11 and 1.12. As it seems reasonable to discuss the theoretical aspects of this results combined with those for the thermal conductivity, we will limit ourselves here to some general observations. We will discuss successively: a the shape of the approach to saturation, b the magnitude of the effect at saturation and finally, c the relative position of the different gases in H/p range.
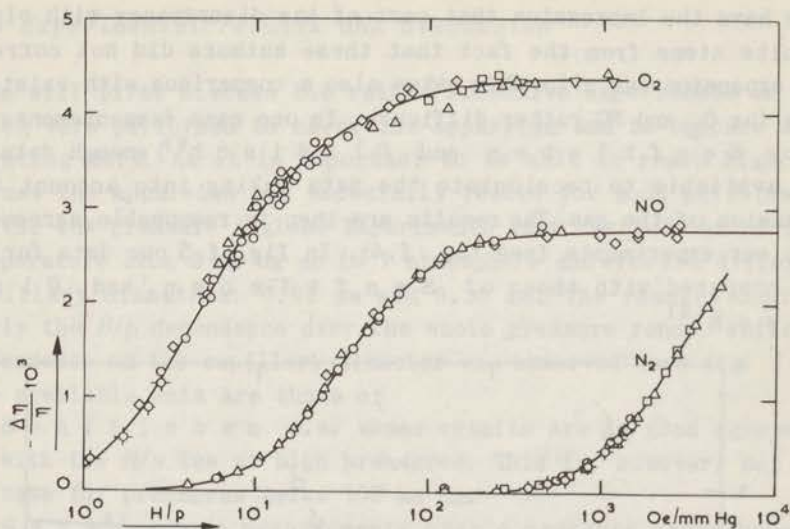
Fig. 1.6

$\Delta \eta / \eta$ as a function of H/p for O_2, NO and N_2.
O_2: capillary diameter 0.96 mm, $\triangle$ 4.6 mm Hg, $\triangle$ 16 mm Hg,
$\diamondsuit$ 120.6 mm Hg, $\circ$ 770 mm Hg; capillary diameter 0.58 mm,
$\square$ 51.1 mm Hg, $\diamondsuit$ 237.5 mm Hg.
NO: $\diamondsuit$ 6.6 mm Hg, $\circ$ 10.8 mm Hg, $\triangle$ 16.3 mm Hg.
N_2: $\triangle$ 6.9 mm Hg, $\square$ 10.3 mm Hg, $\diamondsuit$ 22.4 mm Hg, $\circ$ 22.9 mm Hg.
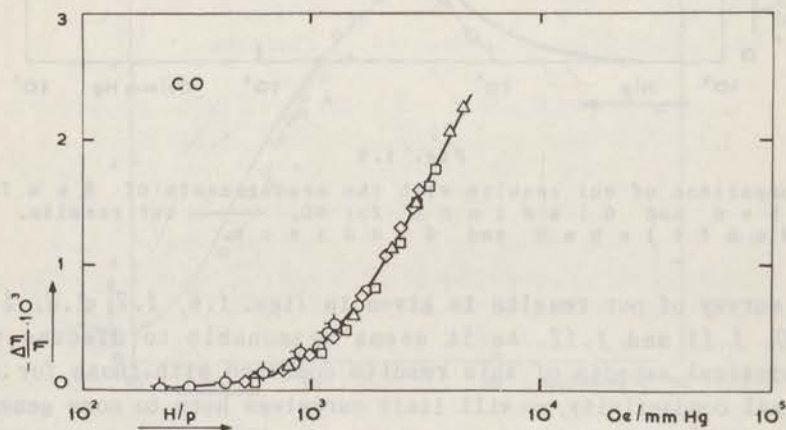
Fig. 1.7

$\Delta \eta / \eta$ as a function of H/p for CO : $\triangle$ 7.1 mm Hg, $\square$ 9.7 Hg,
$\diamondsuit$ 11.1 mm Hg, $\circ$ 19.3 mm Hg, $\diamondsuit$ 26.1 mm Hg.

20
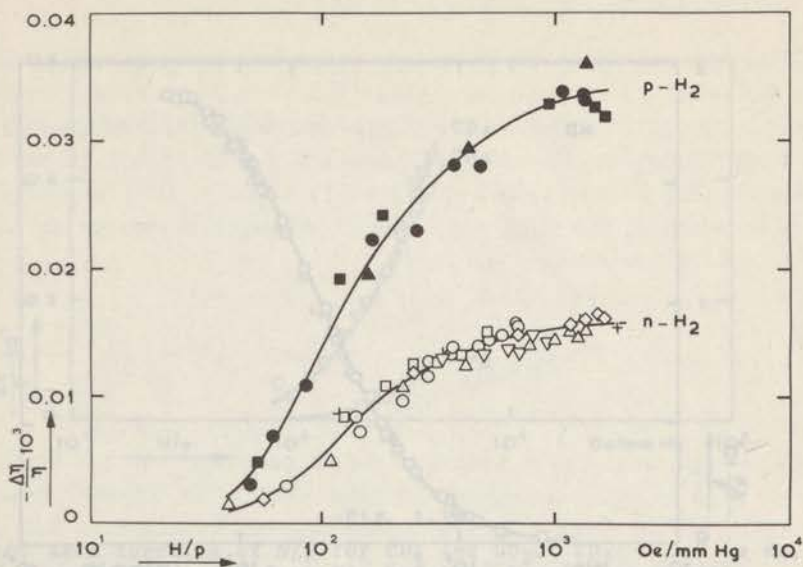
Fig. 1.8

$\Delta \eta / \eta$ as a function of H/p for normal H_2 and para H_2. Normal H_2:
◇ 16.7 mm Hg, ▽ 17 mm Hg, △ 20.1 mm Hg, ○ 23.5 mm Hg, □ 26.9 mm Hg.
Para H_2: ▲ 16 mm Hg, ● 18 mm Hg, ■ 19 mm Hg. Converted para H_2:
+ 17 mm Hg.
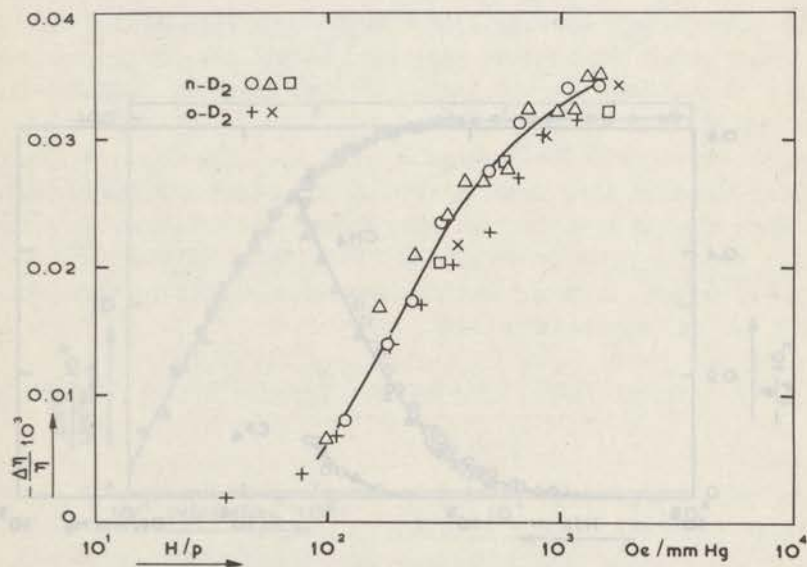
Fig. 1.9

$\Delta \eta / \eta$ as a function of H/p for normal D_2 and ortho D_2.
Normal D_2: ○ 16 mm Hg, △ 19 mm Hg. Ortho D_2: + 17 mm Hg,
× 18 mm Hg. Converted ortho D_2: □ 20 mm Hg.

21
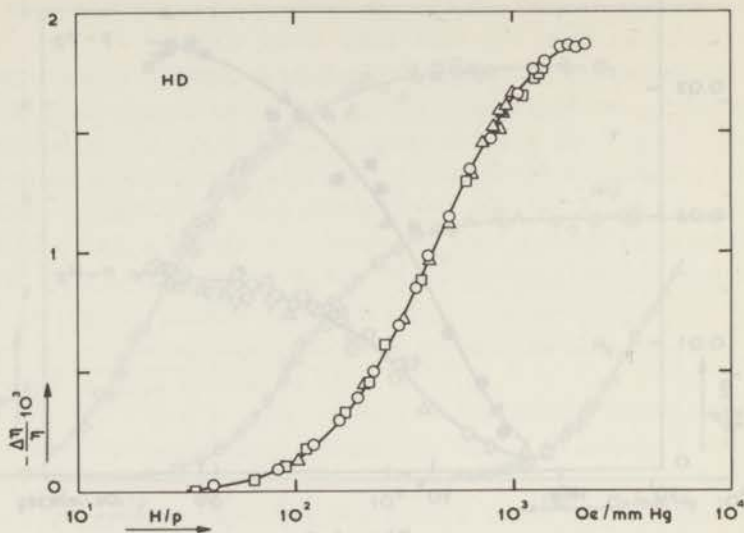
Fig. 1.10

$\Delta \eta/\eta$ as a function of H/p for HD : ○ 15 mm Hg,
□ 17 mm Hg, △ 19 mm Hg.
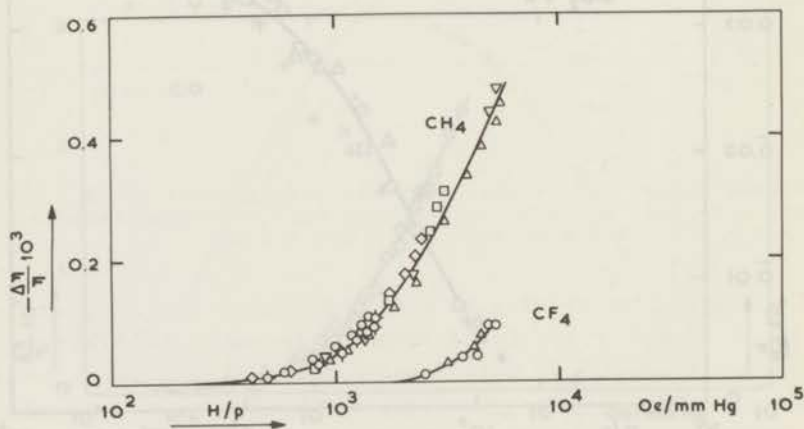
Fig. 1.11

$\Delta\eta/\eta$ as a function of H/p for CH_4 and CF_4. CH_4: △ 6 mm Hg,
▽ 6.2 mm Hg, □ 10.7 mm Hg, ◇ 13.4 mm Hg, ◇ 22.3 mm Hg,
○ 23.5 mm Hg. CF_4: ○ 6.4 mm Hg, △ 7.4 mm Hg.

22
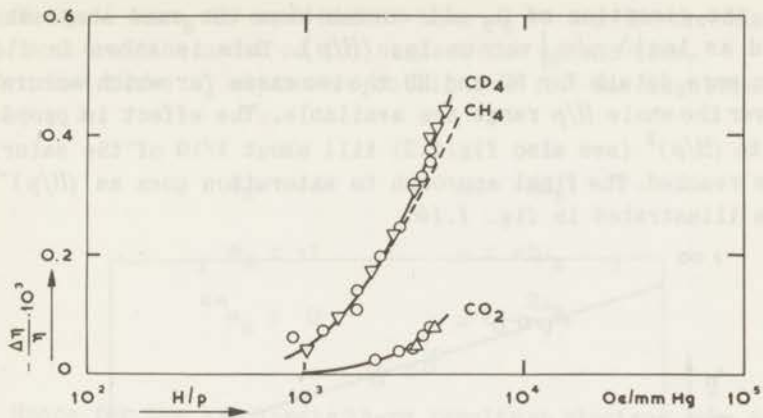
Fig. 1.12

$\Delta\eta/\eta$ as a function of H/p for CD_4 and CO_2. CD_4: ∇ 5.3 mm Hg,
$\circ$ 6.2 mm Hg. CO_2: $\triangle$ 8.5 mm Hg, $\circ$ 8.8 mm Hg. For comparison
----- CH_4.
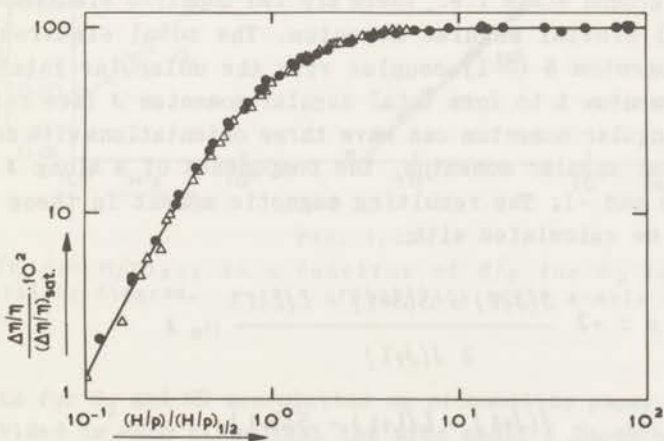
Fig. 1.13

$(\Delta\eta/\eta)/(\Delta\eta/\eta)_{sat}$ as a function of $(H/p)/(H/p)_{1/2}$ on a double
logarithmic scale for NO and HD, $\bullet$ NO : $\triangle$ HD.

23

a With the exception of O_2 all curves have the same shape when plotted as $\log|\Delta\,\eta/\eta_o|$ versus $\log\,(H/p)$. This is shown in fig. *1.13* in more detail for NO and HD the two cases for which accurate data over the whole H/p range are available. The effect is proportional to $(H/p)^2$ (see also fig.*1.2*) till about 1/10 of the saturation is reached. The final approach to saturation goes as $(H/p)^{-2}$. This is illustrated in fig. *1.14*.
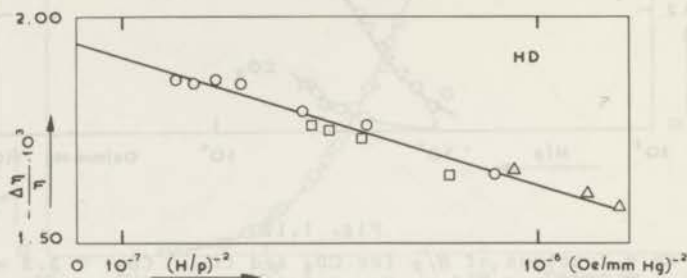
Fig. 1.14

$\Delta\,\eta/\eta$ as a function of $(H/p)^{-2}$ for HD: O 15 mm Hg, □ 17 mm Hg, △ 19 mm Hg.

The curve for O_2 spreads over a much wider range of H/p than for the other gases. This can be explained as follows. O_2 is a molecule with a $^3\Sigma$ ground state i.e., there are two unpaired electrons with zero total orbital angular momentum. The total electron spin angular momentum **S** (S=1) couples with the molecular rotational angular momentum **L** to form total angular momentum **J** (see ref.33). The spin angular momentum can have three orientations with respect to the total angular momentum, the components of **S** along **J** being $m_S = +1$, 0 and -1. The resulting magnetic moment in these three cases can be calculated with

$$\mu = -2\,\frac{J(J{+}1) + S(S{+}1) - L(L{+}1)}{2\,J(J{+}1)}\,\mu_B\,\mathbf{J}$$

$$+\,g\,\frac{J(J{+}1) + L(L{+}1) - S(S{+}1)}{2\,J(J{+}1)}\,\mu_N$$

$$(1.8)$$

where μ_B and μ_N are the Bohr and nuclear magneton respectively. -2 and g are respectively the electron spin and rotational Lande's

g-factor. As μ_B is much higher than μ_N we may in the case of O_2 (J and L of the order of 10) neglect the second term.

For the three m_S states we obtain now for the magnetic moment along J:

$$m_S = +1 \qquad \mu = -2\mu_B$$

$$m_S = -1 \qquad \mu = +2\mu_B \qquad \qquad (1.9)$$

$$m_S = 0 \qquad \mu = -\frac{2\mu_B}{J}$$

Hence for the $m_S = 0$ state there results an electron spin magnetic moment that is about one order of magnitude smaller than in the $m_S = \pm 1$ states. One has to expect that the third of the molecules that are in the $m_S = 0$ state contribute to the changes in the viscosity tensor at appreciably higher fields, giving a spread in the approach to saturation (see also ref. 22). In fig. *1.15* the
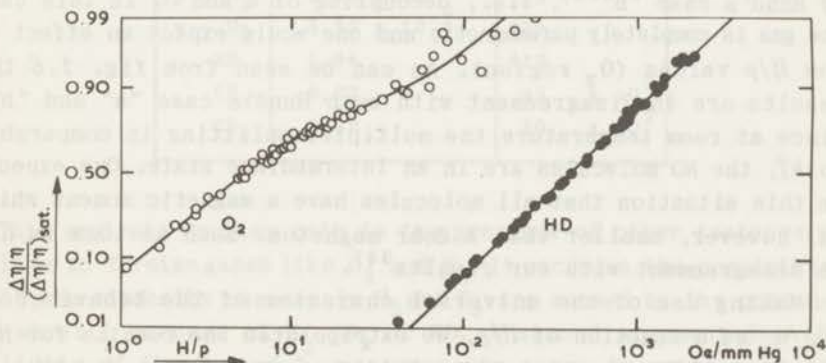
Fig. 1.15

$(\Delta\eta/\eta)/(\Delta\eta/\eta)_{\mathrm{sat}}$ as a function of H/p for O_2 and HD in a probability diagram. y-axis probability scale x-axis logarithmic scale.

results for O_2 and HD are plotted on probability paper. The y-axis is divided in such a way that the area under a Gaussian curve up to the value x plotted versus x becomes a straight line. In the paper we used the x-axis has a logarithmic scale. The advantage of this type of paper is that S-shaped curves will be represented as nearly straight lines. This is indeed the result for HD and

25

other gases. This way of plotting shows clearly that O_2 behaves quite differently.

NO does not show such an effect. The situation here is, however, rather complicated. NO is in a $^2\Pi$ state i.e., there is both an electron spin and an electron orbital magnetic moment. For low rotational quantum numbers, J, of the molecule there is a strong L, S coupling (L is the total orbital and S is the spin quantum number of the electrons) and the $^2\Pi$ state can be described by Hund's case "a"[33]. In this situation NO has a $^2\Pi$ 3/2 state which is paramagnetic and a $^2\Pi$ 1/2 state which is diamagnetic. The magnetic moment in the $^2\Pi$ 3/2 state is about a few hundred times the magnetic moment of the $^2\Pi$ 1/2 state, where it is only brought about by the rotation of the molecule. So one should expect for low enough value of J not only an effect at low H/p values (O_2 region) but also a contribution from the diamagnetic molecules at high H/p values (N_2 region). For high rotational quantum numbers that will be dominant when the multiplet splitting is small compared to kT, the magnetic structure can be described by Hund's case "b"[33], i.e., decoupling of L and S. In this case the gas is completely paramagnetic and one would expect an effect at low H/p values (O_2 region). As can be seen from fig. 1.6 the results are in disagreement with both Hund's case "a" and "b". Since at room temperature the multiplet splitting is comparable to kT, the NO molecules are in an intermediate state. One expects in this situation that all molecules have a magnetic moment which is, however, smaller than a Bohr magneton. Such an idea is not in disagreement with our results[34].

b Making use of the universal character of the behaviour of $\Delta\eta/\eta_0$ as a function of H/p, we extrapolated the results for N_2, CO, CH_4 and CD_4 to saturation. This was not possible for CF_4 and CO_2 as these gases are only measured in the region where $\Delta\eta/\eta_0$ is proportional to $(H/p)^2$. Table $1.II$ contains results of saturation values determined experimentally and by extrapolation. As can be seen, the effects for O_2, NO, N_2 and CO are all of the same order of magnitude. In view of the rather similar physical behaviour of these gases this is not surprising. The change of the viscosity for H_2 and D_2, however, is two orders of magnitude smaller than for O_2 etc.. This is what one should expect qualitatively in view of the fact that the H_2 - H_2 interaction is nearly spherically symmetric. The very small effect for H_2 and D_2 makes it necessary to look more carefully for possible spurious

effects e.g. 1% of HD would give an effect of the same order of magnitude. The purity was determined by performing a thermal diffusion experiment, between 293 and 77°K. No detectable change in the room temperature composition was found after the experiment; this corresponds to a purity of better than 99.7 percent.

Tabel 1.II

gas	$\frac{\Delta\eta}{\eta_0} \, 10^3$ (in saturation)	$(H/p)_{\frac{1}{2}}$ (Oe/mm Hg)
O_2	4.35	5.1
NO	2.77	33.5
N_2	3.0	27.5×10^2
CO	3.75	36.5×10^2
n.- H_2	1.60×10^{-2}	145
p - H_2	3.45×10^{-2}	125
n - D_2	3.50×10^{-2}	220
HD	1.94	410
CH_4	0.77	42×10^2
CD_4	1.02	50×10^2

This analysis applies both to the presence of other isotopes as well as to foreign gases like O_2 and N_2. It excludes the possibility that the viscosity changes in H_2 and D_2 are caused by the presence of about 1 percent of N_2, O_2 or HD. A second argument for the validity of the H_2 and D_2 measurements comes from the range of H/p values in which saturation is reached. This is far different from that found for both O_2 and N_2. Finally, we performed the following check. The experiment was performed with para H_2. Then, by means of a platinum wire that was heated red hot, the para H_2 was converted to normal H_2. The viscosity change measured with this converted gas was equal to that of a separate sample of normal H_2. In conclusion we feel confident that the results shown for H_2 and D_2 are reliable.

The strikingly different behaviour of HD will be related to the asymmetric mass distribution that makes HD behave nearly as a loaded sphere. For a discussion of the properties of loaded sphere

27

molecules see e.g. ref. 35. There is also a difference between normal H_2 and para H_2. In para H_2 which has even rotational quantum numbers, at room temperature about half of the molecules have $J = 0$ and half have $J = 2$. Higher values of J do not appreciably occur. In the case of $J = 0$ the rotational magnetic moment of the molecule is absent, so that only half of the molecules ($J = 2$) will contribute to the effect. In normal H_2 on the other hand, which contains 25% para H_2 only 13% of the molecules will give no contribution. Notwithstanding the fact that in normal H_2 a much larger fraction of the molecules contribute to the effect, the change in the viscosity is much smaller than in the case of para H_2. This shows that the para H_2 molecules in the $J = 2$ state contribute appreciably more than the ortho H_2 molecules which are nearly all in the $J = 1$ state. We come back to this in more detail in chapter III. A similar difference in the behaviour of ortho D_2 and normal D_2 is partially suppressed by the fact that normal D_2 contains already 2/3 ortho D_2.

The results for CH_4 and CD_4 are somewhat smaller than for molecules like N_2. The effect for CD_4 is higher than for CH_4. c Making use of the universal behaviour of the $\Delta \eta/\eta_0$ versus H/p plots, it is possible to determine also the halfway values $(H/p)_{\frac{1}{2}}$, in the case where measurements do not extend up to saturation. $(H/p)_{\frac{1}{2}}$ values for all gases, with the exception of CF_4 and CO_2, are given in table 1.II.

The occurrence of different magnetic moments along the axis of rotation in the $m_S = 0$ and $m_S = \pm 1$ states complicates the interpretation of the $(H/p)_{\frac{1}{2}}$ value for O_2. Still, as far as orders of magnitude are concerned one can safely state that the shift in H/p range between O_2 and N_2 is of the right order viz., μ_B/μ_N. The time scale involved is of the order of the time between two successive collisions. N_2, CO, CH_4 and CD_4 saturate in the same region of H/p. This corresponds qualitatively to the fact that their rotational Lande's g- factors are of the same order.

The H_2-isotopes however, show a different behaviour. The rotational Lande's g- factors for N_2 and H_2 are $g = 0.26$[36] and $g = 0.88$[37] respectively. The difference in magnetic moment is compensated by the fact that the collision frequency for H_2 is higher than for N_2. Thus one might expect the H/p values of importance for N_2 and normal H_2 to be nearly the same. From figs. 1.6 and 1.8, however, we see that normal H_2 is already saturated while N_2 is still far from saturation. This suggests that, at least in the case of H_2,

the characteristic time that corresponds to the collision process that is disturbed is far from ($\approx 10x$) the time between two successive collisions. We will return to this subject in chapter III.

REFERENCES

1. S e n f t l e b e n, H., Phys. Z. 31 (1930) 961.
2. E n g e l h a r d t, H. and S a c k, H., Phys. Z. 33 (1932) 724.
3. S e n f t l e b e n, H. and P i e t z n e r, J., Ann. Phys. 16 (1933) 907.
4. S a c k, H., Helv. Phys. Acta 7 (1934) 639.
5. T r a u t z, M. and F r ö s c h e l, E., Ann. Phys. 22 (1935) 223.
6. S e n f t l e b e n, H. and P i e t z n e r, J., Ann. Phys. 27 (1936) 108.
7. S e n f t l e b e n, H. and P i e t z n e r, J., Ann. Phys. 27 (1936) 117.
8. S e n f t l e b e n, H. and P i e t z n e r, J., Ann. Phys. 30 (1937) 541.
9. S e n f t l e b e n, H. and G l a d i s c h, H., Ann. Phys. 30 (1937) 713.
10. R i e g e r, E., Ann. Phys. 31 (1938) 453.
11. T o r w e g g e, H., Ann. Phys. 33 (1938) 459.
12. S e n f t l e b e n, H. and G l a d i s c h, H., Ann. Phys. 33 (1938) 471.
13. G o r t e r, C.J., Naturwiss. 26 (1938) 140.
14. Z e r n i k e, F. and V a n   L i e r, C., Physica 6 (1939) 961.
15. B e e n a k k e r, J.J.M., S c o l e s, G., K n a a p, H.F.P. and J o n k m a n, R.M., Phys. Letters 2 (1962) 5.
16. W a l d m a n n, L., Z. Naturforschung 12a (1957) 660.
17. W a l d m a n n, L., Z. Naturforschung 13a (1958) 609.
18. W a l d m a n n, L. and K u p a t t, H.D., Z. Naturforschung 18a (1963) 86.

29

19. W a l d m a n n, L., Proc. Intern. Seminar on Transport properties of gases, Providence, (1964) 59.
20. K a g a n, Y. and A f a n a s e v, A.M., Soviet Phys. JETP **14** (1962) 1096.
21. K a g a n, Y. and M a k s i m o v, L., Soviet Phys. JETP **14** (1962) 604.
22. K n a a p, H.F.P. and B e e n a k k e r, J.J.M., Commun. Kamerlingh Onnes Lab. Leiden, Suppl. No. **124**; Physica **32** (1966).
23. K o r v i n g, J., H u l s m a n, H., K n a a p, H.F.P. and B e e n a k k e r, J.J.M., Phys. Letters **17** (1965) 33.
24. De G r o o t, S.R. and M a z u r, P., Non-equilibrium thermodynamics, (North-Holland Publishing Cy., Amsterdam, 1962).
25. K o r v i n g, J., H u l s m a n, H., K n a a p, H.F.P. and B e e n a k k e r, J.J.M., Phys. Letters **21** (1966) 5.
26. B e c k e r, E.W. and S t e h l, O., Z. Phys. **133** (1952) 615.
27. Van E e, H., Thesis Leiden, p. 21 (1966).
28. S c h m i t, G., Thesis Delft, (1945).
29. H o o y m a n, G.J., M a z u r, P. and De G r o o t, S.R., Physica **21** (1955) 355.
30. L o e b, L.B., The kinetic theory of gases, (McGraw Hill Book Cy, Inc. New York and London, 1934), p. 297.
31. K o h l r a u s c h, F., Praktische Physik, (B.G. Teubner Verlagsgesellschaft, Stuttgart, 1955), Band I, p. 159.
32. M e r c e a, V. and U r s u, I., Studii Cercetari Fiz. **2** (1958) 277.
33. H e r z b e r g, G., Molecular spectra and molecular structure, (D. VanNostrand Cy., Inc. Princeton, 1961).
34. D o u s m a n i s, G.C., S a n d e r s, Jr, T.M. and T o w n e s, C.H., Phys. Rev. **100** (1955) 1735.
35. S a n d l e r, S.I., and D a h l e r, J.S., J. chem. Phys. **43** (1965) 1750.
36. C h a n, S.I., B a k e r, M.R. and R a m s e y, N.F., Phys. Rev. **136** (1964) A 1224.
37. H a r r i c k, N.J. and R a m s e y, N.F., Phys. Rev. **88** (1952) 228.

C H A P T E R I I

T H E R M A L   C O N D U C T I V I T Y

2.1 *Introduction*

In chapter $I^{1)}$ we gave a general introduction on the influence
of a magnetic field on the transport properties of polyatomic
molecules. Furthermore experiments were reported on the change of
the viscosity for several gases. Although for monatomic gases
measurements of the thermal conductivity give practically the
same information as viscosity experiments, this is not the case
for polyatomic gases. Here the situation is changed by the presence
of heat transport through the internal degrees of freedom and the
occurrence of inelastic collisions. Hence we decided to study also
the influence of a magnetic field on the thermal conductivity. In
this chapter we will describe the measurements of the change of
the thermal conductivity in a magnetic field for O_2, NO, N_2, CO
and CH_4.

In the same way as in chapter I we will confine ourselves to a
qualitative discussion of the results. A comparison of the data
for thermal conductivity and viscosity with the available theory
will be given in chapter III.

2.2 *Experimental method and apparatus*

a General

A diagram of the apparatus, which consists of two identical
cylindrical cells, is given in fig. *2.1*. One of the cells is filled
with the gas to be investigated while the other, filled with an
inert gas, serves as a reference cell. The measurements were made
in a cylindrical cell with axis normal to the magnetic field
lines. The change in thermal conductivity was obtained by measuring

the change of the temperature gradient in the sample at constant
heat input to the cell. Each cell consisted of a 2 mm diameter
hollow copper rod, C, suspended vertically in the 8 mm cylindrical
cavity of a large brass block. The block was surrounded by a non-
circulating waterbath in a cryostat; this provided a constant
room-temperature bath of large heat capacity. The copper rod could
be heated a few degrees Celsius above the block temberature by
means of the heaters, H, which were attached to the ends of the
rod. This method of heating was chosen over the platinum wire
method employed by S e n f t l e b e n[2], G o r e l i k[3] and
others, for several reasons. First, using the relatively large
diameter of the rod one avoids irregularities in the heat transfer
mechanism near the rod at low gas pressures. In the wire method
the larger part of the temperature gradient extends then over
only a few mean free path lengths. Further, a small electrically
heated wire with axis normal to the magnetic field lines would
be subject to Lorentz force displacements disturbing the symmetry
of the heat fluxes. Finally, this type of design reduces end
corrections in the sample cell. A temperature difference of
approximately 2.5 degrees celsius was maintained between the rod
and the block, with nitrogen as the sample gas and a heat input
of about 10 milliwatt.

The change in thermal conductivity caused by the field was
indicated by a change in temperature of the copper rod. Negative
temperature coefficient thermistors, T, attached to the rod and
the block provided the temperature measurements. The resistance
of the rod thermistor was measured differentially in a Wheatstone
bridge against the rod thermistor of an identical cell adjacent
to the measuring cell in the block. The comparison cell contained
a monatomic gas whose thermal conductivity was, of course,
unaffected by the presence of the magnetic field. The thermal
conductivity of the comparison gas was chosen close to that of the
measured gas so that transport conditions in the comparison cell
closely resembled those in the measuring cell. The use of this
differential measuring method permitted compensation of all
influences on the measured gas except the magnetic field effects.
Because of the lack of perfect similarity of the thermistors, a
small correction had to be applied at high fields. There were no
observable field effects on the heaters.

Thermistors with resistances of 15 k Ω and temperature coeffi-
cients of 6% per degree Celsius were employed. The unbalance of

32

the Wheatstone bridge in the presence of a magnetic field was measured, after amplification, with a chart recorder. Electronic instabilities limited the detectable temperature changes to about 4×10^{-4} °C. The measurements are time consuming because of the rather slow response of the cell. Measurements with either helium or argon in the two cells yielded no effect in the presence of a magnetic field.

b Details of cell design

The gas sample was confined to the central 35 mm portion of the copper rod by the vacuum seals (described below). The heaters and thermistor were attached to the extremes of the rod, which were thermally isolated from the block by high vacuum. The vacuum communicated from above to the underside of the cell through the 1 mm hole in the copper rod. The upper end of the cell was pumped directly through pumping lines, P, of 10 mm thin walled, new silver tubing. The tubes, one each to the measuring and comparison cells in the block, also provided physical support for the block in the bath.

The sample gas was introduced into the cell through a 0.5 mm hole in the brass block. The new silver inlet tube, F, connected the block to the pumping system and to an oil manometer with which the pressure in the cell was measured.

The vacuum seals on the cell were designed to reduce as much as possible the heat leak from the rod to the block. A thin-walled glass cylinder, G, and a slightly larger new silver tube, N, were placed concentric to the copper rod to increase the heat resistance of each seal (see fig. 2.1). The ends of the glass tube, which itself was 2.40 mm i.d. and 3.1 mm o.d., were sealed to the copper rod and new silver tube (3.8 mm i.d.) with short sections of platinum tubing. The seal was completed with a new silver disc, D (0.2 mm thick), soldered to the free end of the new silver tube. The disc was sealed to the block by Indium "O" rings, I, as shown in the figure. Vacuum tests proved that no gas was leaking from the cell into the pumping line.

At sample pressures well above the Knudsen region all the heat from the rod into the seals passes through the gas between the new silver and glass tubes. In the Knudsen range, however, the heat transfer occurs mostly through the long glass tube which has high thermal resistance. Thus, at all operating pressures the effective conductivity of the seal is small.

P
T
H
F
N
G
I
D
T
C
I
Pt
H
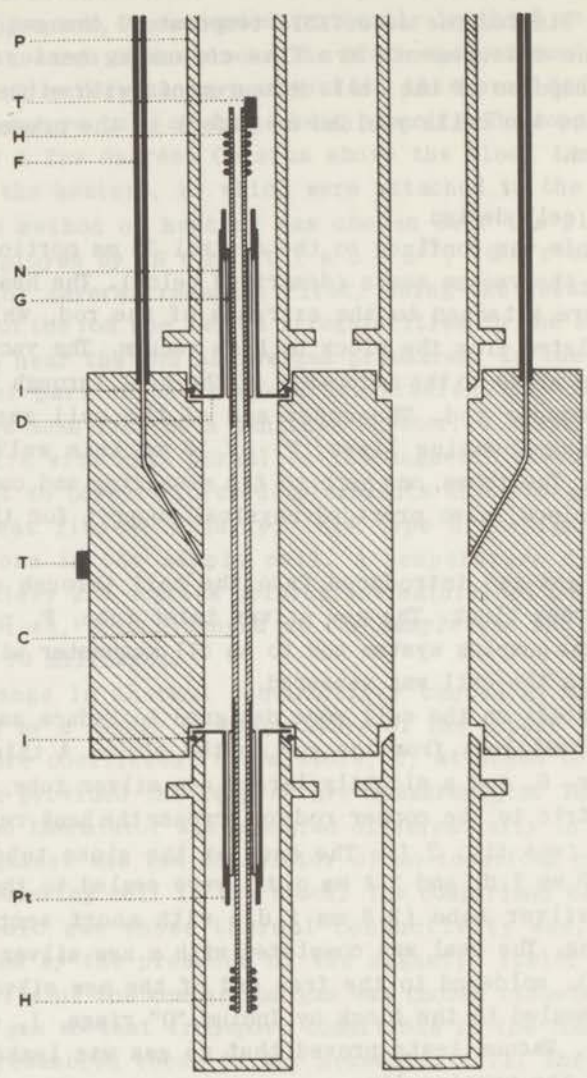
Fig. 2.1
A schematic diagram of the apparatus.

34

In table 2.I the purity and origin of the gases studied are given.

Table 2.I

gas	origin	purity	main impurities if known
O_2	commercial	99.95%	
NO	commercial	99. %	0.4% CO_2
N_2	commercial	99.95%	
CO	commercial	98 %	0.5% N_2
CH_4	commercial	98 %	1 % N_2, CO

2.3 *Calculation of the results*

In the field free case the heat flow, **q**, between two coaxial cylinders of infinite length can be calculated from

$$\text{div } \mathbf{q} = 0$$

with

$$q_x = -\lambda_o \frac{\partial T}{\partial x}; \quad q_y = -\lambda_o \frac{\partial T}{\partial y}; \quad q_z = 0$$

(2.1)

The boundary conditions are $T(R_1) = T_1$; $T(R_2) = T_2$; R_1 and R_2 are the inner and outer radius of the cell (see fig. 2.2).
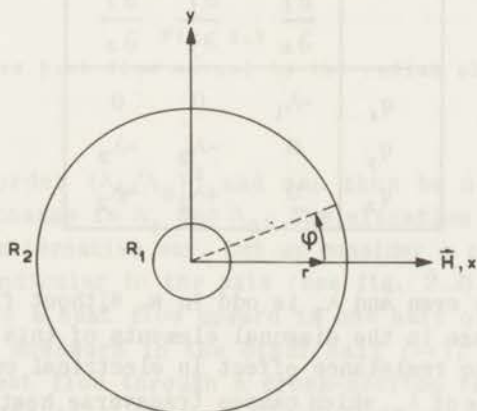
Fig. 2.2
Cross-section of the cell in the radial plane.

The result is a cylindrically symmetric solution for T as a function of position r:

$$T = T_1 - \frac{T_1 - T_2}{\ln(R_2/R_1)} \ln(r/R_1)$$ (2.2)

so that the radial heat flow per unit length, Q_r, is given by

$$Q_r = - \int_0^{2\pi} \lambda_o \frac{\partial T}{\partial r} r \, d\phi = \frac{2\pi\lambda_o}{\ln(R_2/R_1)} (T_1 - T_2)$$ (2.3)

In the presence of a magnetic field, however, the situation is more complicated. As we have seen already in chapter I, a magnetic field changes the description of the transport phenomenon so that we have

$$q_i = - \sum_k \lambda_{ik} \frac{\partial T}{\partial x_k}$$ (2.4)

Using space symmetry relations only one can easily show that the thermal conductivity tensor, λ_{ik}, in a magnetic field can be written as (the direction of the field, H, is taken as the x-axis) [4]

	$\dfrac{\partial T}{\partial x}$	$\dfrac{\partial T}{\partial y}$	$\dfrac{\partial T}{\partial z}$
q_x	$-\lambda_1$	0	0
q_y	0	$-\lambda_2$	$-\lambda_3$
q_z	0	$+\lambda_3$	$-\lambda_2$

(2.5)

λ_1 and λ_2 are even and λ_3 is odd in H. Without field $\lambda_1 = \lambda_2 = \lambda_o$ and $\lambda_3 = 0$. The change in the diagonal elements of this scheme is similar to the magneto resistance effect in electrical conductivity while the occurrence of λ_3, which causes transverse heat flow perpendicular to the temperature gradient and field direction, is analogous to the Hall effect. Till recently this transverse heat flow was

36

only observed in metals, where it is known as the Righi-Leduc effect. Preliminary experiments show that this transverse heat flow occurs also in polyatomic gases[5]. We found that, as in the case of viscosity, the off-diagonal elements are of the same order of magnitude as the change caused by a field in the diagonal elements. As a result one has, if one measures the change of the diagonal elements, to consider a possible influence of transverse heat flow in the cell experiments. In our cylindrically symmetric set-up, which has the field perpendicular to the axis of symmetry the thermal resistance has to be even in the direction of H. Hence a contribution to the radial heat flow from λ_3, which is odd in H,
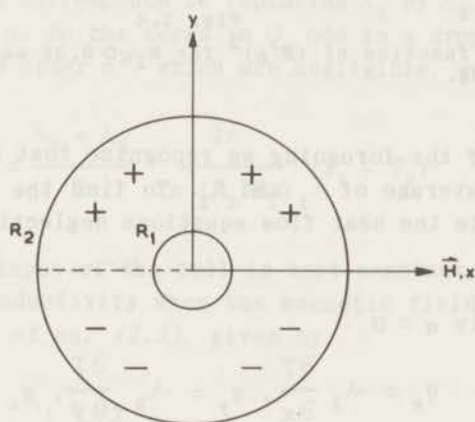
Fig. 2.3

Transverse heat flow normal to the radial plane.

will be of the order $(\lambda_3/\lambda_0)^2$ and can thus be neglected as compared to the change in λ_1 and λ_2. The situation can also be elucidated in an alternative way. Let us consider a cross-section of the cell perpendicular to the axis (see fig. 2.3). Transverse effects will cause a heat flow upward in one half of the cross-section (++) and downward in the other half (--). It is clear that the total heat flow through a cross-section remains zero. Higher order terms in λ_3/λ_0 can occur through end effects. Experimentally this is confirmed since one finds for N_2 that $\Delta\lambda/\lambda_0$ starts as $(H/p)^2$ (see fig. 2.4).

37
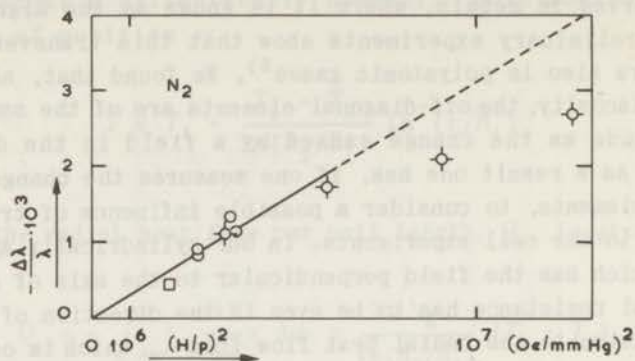
Fig. 2.4

$\Delta \lambda / \lambda$ as a function of $(H/p)^2$ for N_2. $\bigcirc$ 9.28 mm Hg, $\diamondsuit$ 5.09 mm Hg, $\square$ 1.06 mm Hg.

In view of the foregoing we recognize that experimentally we measure an average of λ_1 and λ_2. To find the specific relationship we write the heat flow equations neglecting the transverse terms:

$$\text{div } q = 0$$

where now $\qquad q_x = -\lambda_1 \dfrac{\partial T}{\partial x}, \; q_y = -\lambda_2 \dfrac{\partial T}{\partial y}, \; q_z = 0$ $\qquad (2.6)$

and with the same boundary conditions as before.

Hence $\qquad \text{div } q = -\dfrac{\lambda_1 + \lambda_2}{2} \left(\dfrac{\partial^2 T}{\partial x^2} + \dfrac{\partial^2 T}{\partial y^2} \right) - \dfrac{\lambda_1 - \lambda_2}{2} \left(\dfrac{\partial^2 T}{\partial x^2} - \dfrac{\partial^2 T}{\partial y^2} \right) = 0 \qquad (2.7)$

As the second term of the lefthand side of eq. (2.7) is a small perturbation, we develop the solution for T in a power series in $(\lambda_1 - \lambda_2)/(\lambda_1 + \lambda_2)$:

$$T = T^{(0)} + a \, T^{(1)} + a^2 \, T^{(2)} + \ldots \qquad a = \dfrac{\lambda_1 - \lambda_2}{\lambda_1 + \lambda_2} \qquad (2.8)$$

where $T^{(0)}$ is the isotropic solution given by formula (2.2) and

38

$T^{(1)}$ is a deviation caused by the anisotropy in λ : $T^{(1)}(r,\phi)$; ϕ is the azimuthal angle in the radial plane. The radial heat flow per unit length is given by

$$Q_r = \int_0^{2\pi} \{ - (\lambda_1 \cos^2\phi + \lambda_2 \sin^2\phi)\, \frac{\partial T}{\partial r} + \alpha(\lambda_1 + \lambda_2)\, \frac{\sin\phi\, \cos\phi}{r}\, \frac{\partial T}{\partial \phi} \} r\,d\phi \quad (2.9)$$

substituting (2.8) we get

$$Q_r = Q_r^{(0)} + \alpha\, Q_r^{(1)} + \alpha^2\, Q_r^{(2)} + \cdots$$

Turning the magnet over $90°$ in the radial plane does not change Q_r. This operation corresponds to replacing λ_1 by λ_2, i.e., to a change in sign of α. So the terms in Q_r odd in α drop out. Hence up to terms of the order α^2, which are negligible, we have

$$Q_r = \frac{\lambda_1 + \lambda_2}{2} \; \frac{2\pi}{\ln\,(R_2/R_1)} \; (T_1 - T_2) \quad\quad (2.10)$$

Since the heat input of the cell is kept constant, the change of the thermal conductivity when the magnetic field is applied is, with the help of eq. (2.3), given by

$$\frac{\Delta\lambda}{\lambda_0} = \frac{\dfrac{\lambda_1 + \lambda_2}{2} - \lambda_0}{\lambda_0} = - \frac{\delta T}{\Delta T} \quad\quad (2.11)$$

where δT is the increase in temperature of the rod under the influence of the field and $\Delta T = T_1 - T_2$.

The total heat flow in our cell, however, is not only connected to the thermal conductivity of the gas, but also involves additional heat transfer, e.g., by radiation and by conduction through the electrical leads. The situation is further complicated by Knudsen effects at low pressures which give rise to the well known temperature jump at the wall. So, formula (2.11) must be rewritten as

$$\frac{\Delta\lambda}{\lambda_0} = - f\, \frac{\delta T}{\Delta T} \quad\quad (2.12)$$

39

In order to calculate f we will write down the effective thermal conductivity of the cell as follows

$$\frac{Q}{\Delta T} = \frac{1}{R_{cell}} + \frac{1}{R_{seals}} + \frac{1}{R_{other}} \qquad (2.13)$$

Q is the total heat input per unit time, R_{cell} and R_{seals} are the thermal resistances of the gas and the seals respectively, while R_{other} contains all other possible heat losses. R_{cell} is given by

$$R_{cell} = \frac{\ln\ (R_2/R_1)}{2\pi L \lambda_o} + \frac{g_c\ (\frac{1}{R_1} + \frac{1}{R_2})}{2\pi L\ p} \qquad (2.14)$$

(see also ref. 6)

R_1 and R_2 are the radii of the rod and the cell respectively, L is the length of the cell, p the pressure of the gas and g is related to the temperature jump at the wall.

$$R_{seals} = \frac{1}{2}\sqrt{R_g\ R_s} \qquad \text{(see appendix)} \qquad (2.15)$$

R_g is the thermal resistance of the glass tube and R_s is the thermal resistance of the gas in the seals, given by

$$R_s = \frac{\ln\ (r_2/r_1)}{2\pi l \lambda_o} + \frac{g_s\ (\frac{1}{r_1} + \frac{1}{r_2})}{2\pi l\ p} \qquad (2.16)$$

r_1 is the outher radius of the glass tube, r_2 the inner radius of the new silver tube and l is the length of the seal. g_s is the effective value of g for the seals arising from contributions of both the accomodation coefficients of the glass and the new silver surfaces in the seals. R_{other} can be calculated to a good approximation with the help of measurements of $Q/\Delta T$ in vacuum and can be considered as a constant in our measurements.

In the magnetic field the thermal conductivity changes and

40

consequently the rod temperature, T_1, will change. Variation of λ and T_1 in (2.13) at constant Q leads to

$$\frac{\Delta\lambda}{\lambda_o} = -f\frac{\delta T}{\Delta T} = \frac{Q/\Delta T}{\lambda_o\left[\left(\frac{\partial R_{cell}}{\partial\lambda}\right)\Big/R_{cell}^2 + \left(\frac{\partial R_{seals}}{\partial\lambda}\right)\Big/R_{seals}^2\right]}\frac{\delta T}{\Delta T} \qquad (2.17)$$

A change in g and λ as a consequence of a change in T_1, can be neglected since it gives only rise to a correction in f of the order of $\Delta T/T_1$.

In principle the correction factor f is now known, except for the fact that no reliable theoretical expression for g is available. For this reason the denominater of (2.17) will be expressed as far as possible in quantities that can be directly determined by experiment. We therefore introduce the experimental accessible quantity W:

$$W = \frac{Q}{\Delta T} - \frac{1}{R_{other}} \qquad (2.18)$$

It can be easily verified with the help of (2.14), (2.16) and (2.18) that the denominator of (2.17) can be written as

$$-\lambda_o\left[\left(\frac{\partial R_{cell}}{\partial\lambda}\right)\Big/R_{cell}^2 + \left(\frac{\partial R_{seals}}{\partial\lambda}\right)\Big/R_{seals}^2\right] = W + \frac{1}{p}\frac{\partial W}{\partial(1/p)} - \frac{1}{2R_{seals}} \qquad (2.19)$$

Hence we have for f

$$f = \frac{Q/\Delta T}{W + \dfrac{1}{p}\dfrac{\partial W}{\partial(1/p)} - \dfrac{1}{2R_{seals}}} \qquad (2.20)$$

Since $1/2R_{seals} \ll W + (1/p)(\partial W/\partial(1/p))$, the value of f is mainly determined by experimentally accessible quantities. To calculate R_{seals} we have to determine the value of g_s in eq. (2.16). This can be obtained approximately from a plot of $1/W$ versus $1/p$. From

41

(2.14) and (2.16) it follows that such a plot gives for not too low pressures, a straight line (see fig. 2.5), with a slope proportional to g if one assumes $g_c = g_s$. Using this value of g, R_{seals} can be calculated and f is known. f ranges from 1.5 at high pressures (negligible temperature jump) to around 2 at low pressures. When g is expressed in terms of the mean free path in the gas one finds that g corresponds to two or three times the mean free path, which is in reasonable agreement with what one should expect (see e.g. ref. 6). As we indeed found $1/W$ proportional to $1/p$ the occurrence of convection in the cell is ruled out.
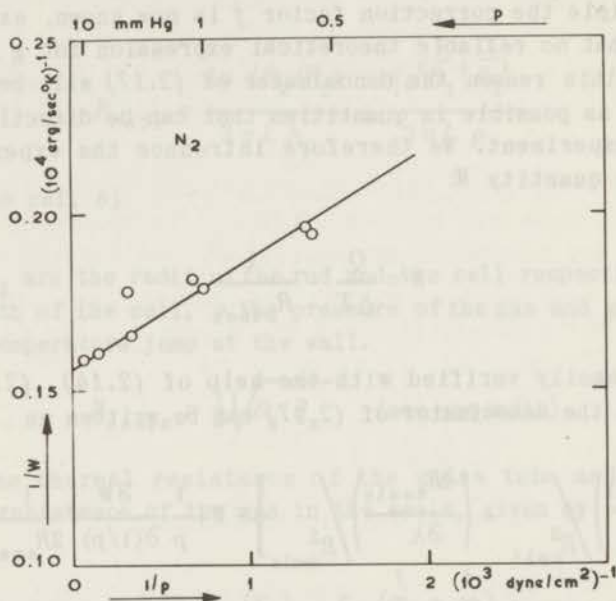
Fig. 2.5

$1/W$ as a function of $1/p$ for N_2.

A further advantage of making such a plot of $1/W$ is that the thermal conductivity of the gas can be calculated directly from the intersection at $(1/p) = 0$. By comparing the value of λ_o so obtained with the known values we are able to check the reliability of our set up. We refer to table 2.II for comparison of λ_o with data from the literature [7, 8]; the agreement is satisfactorily.

Table 2.II

gas	thermal conductivity (10^3erg/s cm $^\circ$K)	
	literature	this experiment
O_2	2.59	2.61
NO	2.51	2.40
N_2	2.53	2.51
CO	2.44	2.28
CH_4	3.29	3.15

This procedure makes it possible to determine the change of the thermal conductivity in a magnetic field with an estimated accuracy of 5%.

2.4 *Experimental results and discussion*

The results of our experiments on O_2, NO, N_2, CO and CH_4 are given in figs. 2.6, 2.7, 2.8, 2.9 and 2.10. A comparison of our results for O_2 and NO is only possible with those of S e n f t - l e b e n and P i e t z n e r (O_2)[9] and T o r w e g g e (NO)[10] and is given in fig. 2.11. The difference in magnitude of the effect between both groups of experiments is rather large. We have however the impression that the analysis of the electrical circuit used by S e n f t l e b e n and P i e t z n e r, was not correct[11][12]. This might explain the discrepancy with our results. The difference in the case of NO (T o r w e g g e) is smaller, about 15%. As it is not clear how they calculated their results it is not possible to come to a definite conclusion on the origin of the discrepancy. While our experiments were in progress G o r e l i k and S i n i t s y n[13] published data on the influence of a magnetic field on the thermal conductivity of N_2, CO, CO_2, H_2 and D_2. A comparison with our results for N_2 and CO is given in fig. 2.12. They used a hot wire method and worked at rather low pressures (0.1 - 0.01 mm Hg). They calibrated their apparatus with O_2 using as a standard the data of S e n f t - l e b e n and P i e t z n e r. Thus, one expects their results to be higher by a factor corresponding to the ratio between our

results for O_2 and those of S e n f t l e b e n and P i e t z-
n e r. This is indeed the case. For a discussion of the results
for H_2 and D_2 see chapter III.
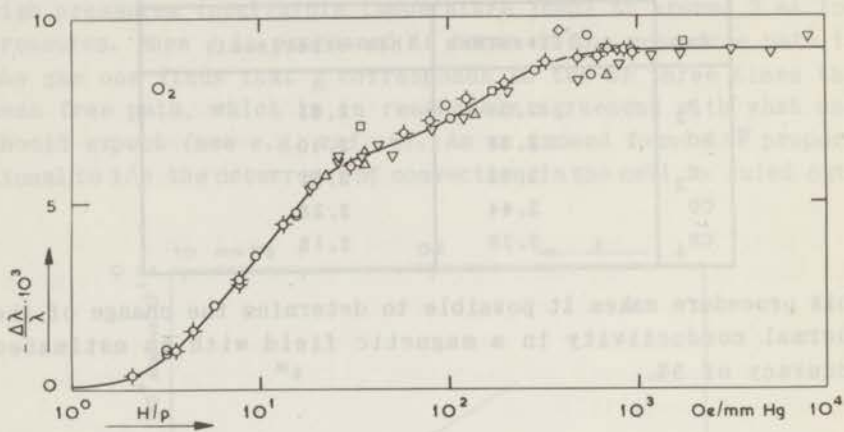
Fig. 2.6

$\Delta \lambda / \lambda$ as a function of H/p for O_2. ○ 31.7 mm Hg, ◇ 19.3 mm Hg,
□ 9.34 mm Hg, ◇ 4.10 mm Hg, △ 2.33 mm Hg, ▽ 1.99 mm Hg.
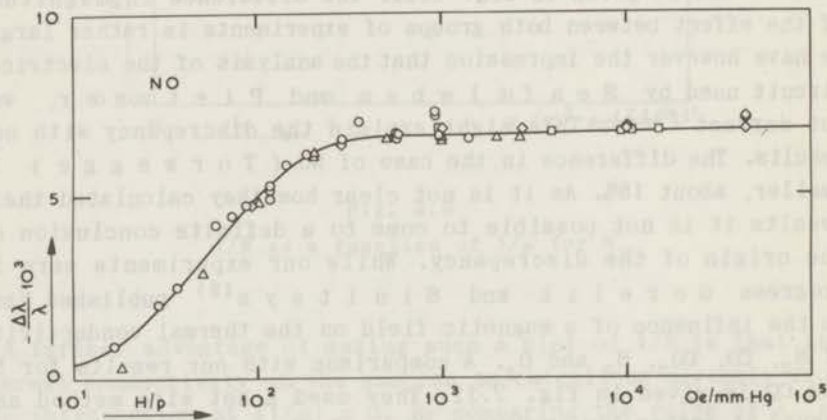
Fig. 2.7

$\Delta \lambda / \lambda$ as a function of H/p for NO. ○ 11.01 mm Hg, △ 6.34 mm Hg,
□ 1.18 mm Hg, ◇ 0.40 mm Hg.

44
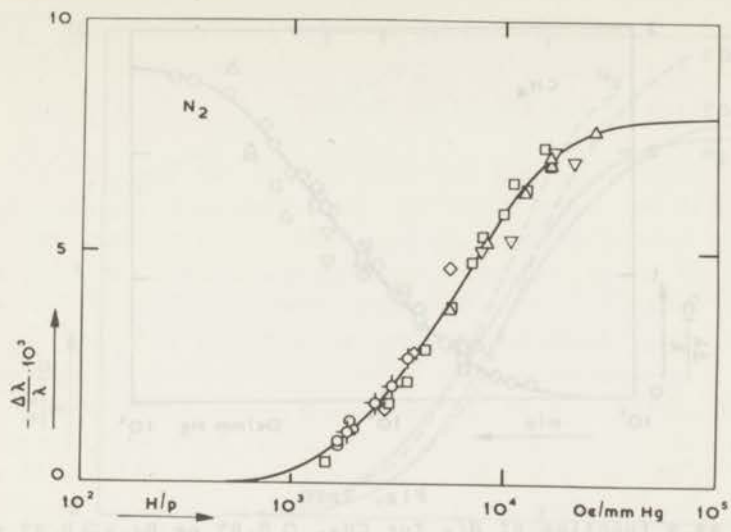
Fig. 2.8

$\Delta\lambda/\lambda$ as a function of H/p for N_2. ○ 9.28 mm Hg, ◇ 5.09 mm Hg, ◇ 2.27 mm Hg, □ 1.06 mm Hg, △ 0.57 mm Hg, ▽ 0.56 mm Hg.
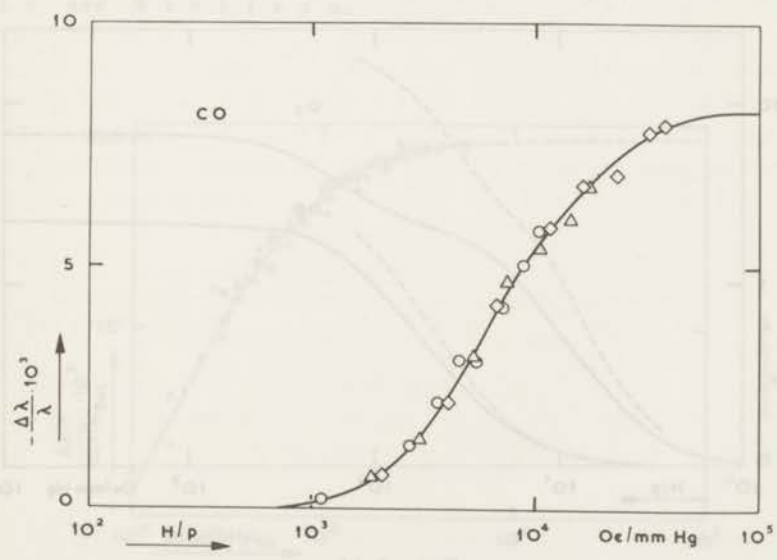
Fig. 2.9

$\Delta\lambda/\lambda$ as a function of H/p for CO. ○ 1.74 mm Hg, △ 1.05 mm Hg, ◇ 0.47 mm Hg.

45
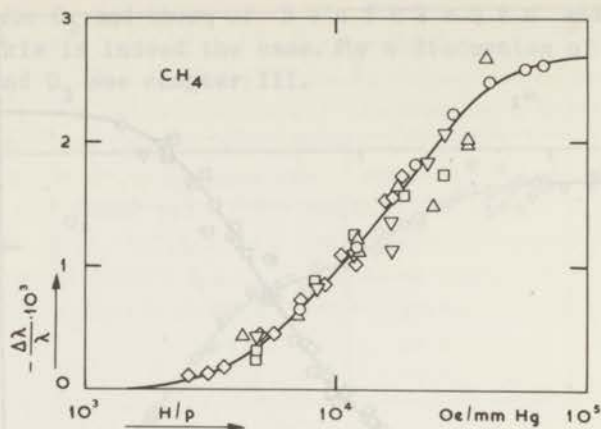
Fig. 2.10

$\triangle$ λ/λ as a function of H/p for CH_4. $\diamond$ 0.97 mm Hg, $\square$ 0.67 mm Hg, $\triangledown$ 0.66 mm Hg, $\triangle$ 0.45 mm Hg, $\bigcirc$ 0.27 mm Hg.
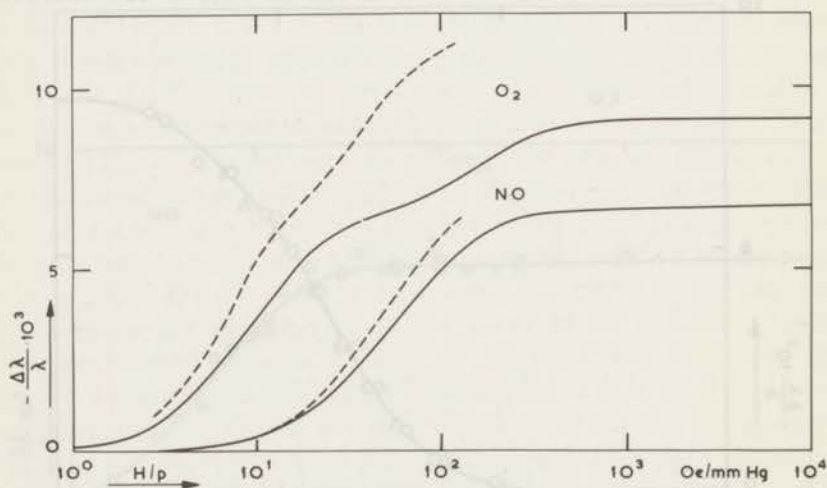
Fig. 2.11

A comparison of our results with those of S e n f t l e b e n and P i e t z n e r for O_2 and those of T o r w e g g e for NO. ——— our results, ----- S e n f t l e b e n and P i e t z n e r (O_2), ----- T o r w e g g e (NO).

46
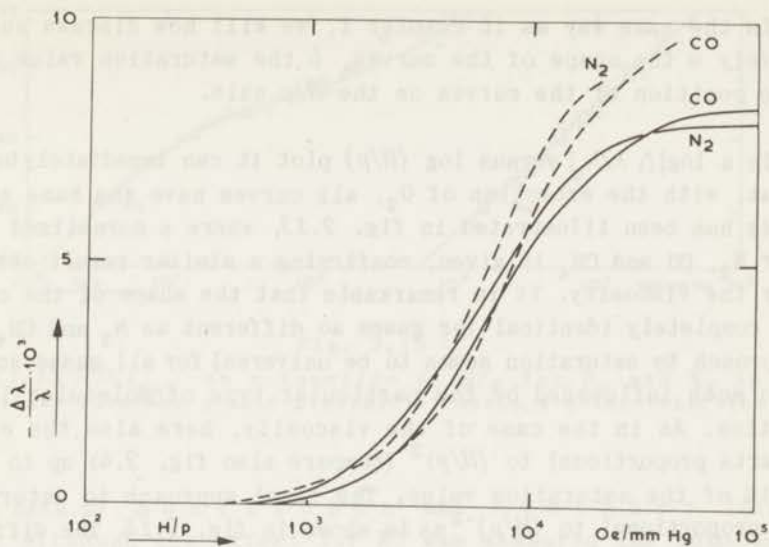
Fig. 2.12

A comparison of our results for N_2 and CO with those of G o r e -
l i k and S i n i t s y n. ———— our results, ----- G o r e -
l i k and S i n i t s y n.
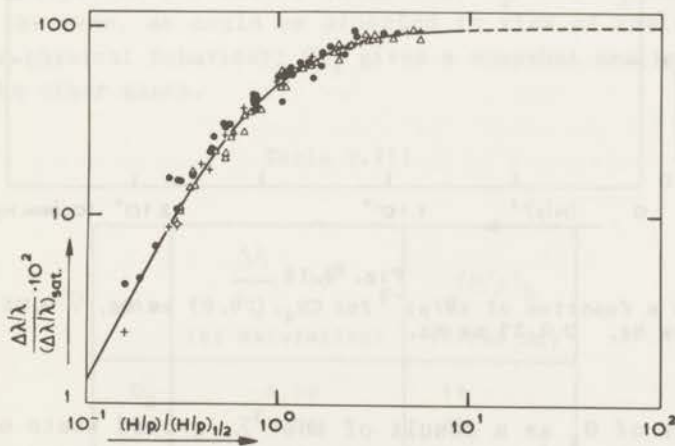
Fig. 2.13

$(\Delta\lambda/\lambda)/(\Delta\lambda/\lambda)_{sat}$ as a function of $(H/p)/(H/p)_{1/2}$ on a double loga-
rithmic scale for N_2, CO and CH_4. $\triangle$ N_2, + CO, ● CH_4.

47

In the same way as in chapter I, we will now discuss succes-
sively a the shape of the curves, b the saturation value and c
the position of the curves on the H/p axis.

a In a $\log|\Delta\lambda/\lambda_0|$ versus $\log (H/p)$ plot it can immediately be seen
that, with the exception of O_2, all curves have the same shape.
This has been illustrated in fig. 2.13, where a normalized curve
for N_2, CO and CH_4 is given, confirming a similar result obtained
for the viscosity. It is remarkable that the shape of the curves
is completely identical for gases so different as N_2 and CH_4. The
approach to saturation seems to be universal for all gases and not
too much influenced by the particular type of molecular inter-
action. As in the case of the viscosity, here also the effect
starts proportional to $(H/p)^2$ (compare also fig. 2.4) up to about
1/10 of the saturation value. The final approach to saturation
is proportional to $(H/p)^{-2}$ as is shown in fig. 2.14. The different
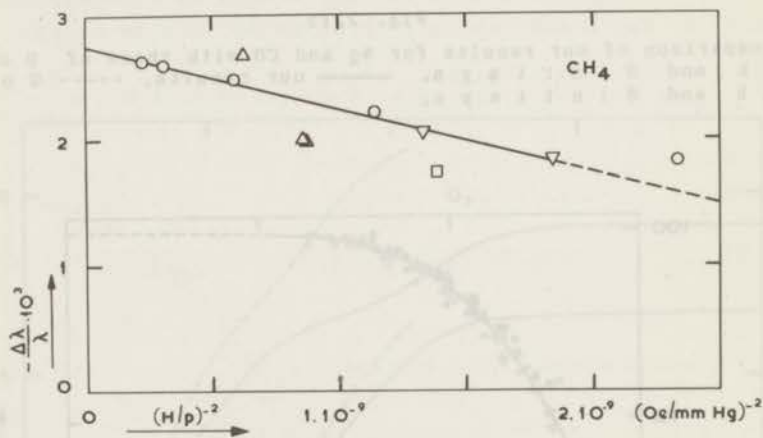
Fig. 2.14
$\Delta\lambda/\lambda$ as a function of $(H/p)^{-2}$ for CH_4. $\square$ 0.67 mm Hg, ∇ 0.66 mm Hg,
$\triangle$ 0.45 mm Hg, $\bigcirc$ 0.27 mm Hg.

behaviour of O_2 as a result of the $^3\Sigma$ ground state of the
molecule - see chapter I - is more pronounced. The molecules in
the $m_S = 0$ state even give rise to a hump in curve. This is shown
more explicitly in fig. 2.15, where the results for O_2 and N_2
are plotted on probability paper. Note that this hump also occurs

48
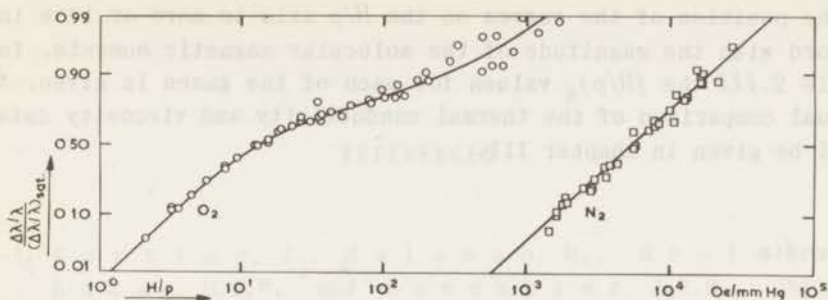
$(\Delta \lambda/\lambda)/(\Delta \lambda/\lambda)_{sat}$ as a function of H/p for O_2 and N_2 in a probability diagram. y-axis probability scale, x-axis logarithmic scale.

in the data by S e n f t l e b e n and P i e t z n e r (fig. 2.11). Although the effect for NO was measured far into the saturation, no effect of a diamagnetic state in NO at room temperature was found as should be expected (see chapter I).

b Since one can make use of the universal behaviour of $\Delta \lambda/\lambda_o$ as a function of H/p, the saturation value can, if necessary, be obtained by extrapolation. The saturation values are given in table 2.III. The saturation values for O_2, NO, N_2 and CO are about the same, as could be expected in view of their rather similar physical behaviour; CH_4 gives a somewhat smaller result than the other gases.

Table 2.III

gas	$\dfrac{\Delta \lambda}{\lambda_o} \, 10^3$ (at saturation)	$(H/p)_{½}$ (Oe/mm Hg)
O_2	9.10	14
NO	6.75	53
N_2	7.90	53×10^2
CO	8.20	69×10^2
CH_4	2.75	157×10^2

c The position of the curves on the H/p axis is more or less in accord with the magnitude of the molecular magnetic moments. In table 2.*III* the $(H/p)_{\frac{1}{2}}$ values for each of the gases is given. A mutual comparison of the thermal conductivity and viscosity data will be given in chapter III.

Appendix

An exact calculation of R_{seals} is, as a result of the complicated structure of the seals (see fig. 2.*1*), rather difficult. The problem is, however, simplified by the fact that the thermal resistance in the vertical, z, direction is mainly determined by the glass tube, G, while the gas between the glass tube and the new silver tube, N, determines the radial thermal resistance. In this approximation one can derive the following differential equation:

$$\frac{\partial^2 \theta}{\partial \zeta^2} = N^2$$

where (2.21)

$$\theta = \frac{T - T_2}{T_1 - T_2} \quad \text{and} \quad \zeta = \frac{z}{l}$$

with boundary conditions $\theta(0) = 1$ and $\theta(1) = 0$. T_1 is the rod temperature, T_2 the bath temperature, $T_2 < T < T_1$ and l is the length of the glass tube. $N^2 = R_g/R_s$; R_g is the thermal resistance of the glass tube and R_s is given by eq. *(2.16)*. After some calculations one finds that

$$\theta = \cosh N \zeta - \coth N \sinh N \zeta \qquad (2.22)$$

and $$\frac{Q_{seals}}{\Delta T} = \frac{1}{R_{seals}} = -\frac{2}{R_g}\left(\frac{\partial \theta}{\partial \zeta}\right)_{\zeta=0} = \frac{2N \coth N}{R_g} \qquad (2.23)$$

under our conditions $\coth N \approx 1$, so that R_{seals} is given by

$$R_{seals} = \frac{1}{2}\sqrt{R_g R_s} \qquad (2.24)$$

REFERENCES

1. K o r v i n g, J., H u l s m a n, H., S c o l e s, G., K n a a p, H.F.P. and B e e n a k k e r, J.J.M., Physica (to be published).

2. S e n f t l e b e n, H., Phys. Z. **31** (1930) 961.

3. G o r e l i k, L.L. and S i n i t s y n, V.V., Soviet Phys. JETP **19** (1964) 272.

4. D e G r o o t, S.R. and M a z u r, P., Non-equilibrium thermodynamics, (North-Holland Publishing Cy., Amsterdam, 1962) p. 235.

5. K o r v i n g, J., H u l s m a n, H., H e r m a n s, L.J.F., D e G r o o t, J.J., K n a a p, H.F.P. and B e e n a k k e r, J.J.M., J. Mol. Spec. **20** (1966) 294.

6. K e n n a r d, E.H., Kinetic theory of gases, (McGraw Hill Book Cy. Inc, New York and London, 1938) p. 177.

7. J o h n s t o n, H.L. and G r i l l y, E.R., J. chem. Phys. **14** (1946) 233.

8. H i l s e n r a t h, J., e.a., Circular 564 of the Nat. Bur. Stand. (1955).

9. S e n f t l e b e n, H. and P i e t z n e r, J., Ann. Phys. **27** (1936) 108.

10. T o r w e g g e, H., Ann. Phys. **33** (1938) 459.

11. S e n f t l e b e n, H. and R i e c h e m e i e r, O., Ann. Phys. **6** (1930) 105.

12. S e n f t l e b e n, H. and P i e t z n e r, J., Ann. Phys. **16** (1933) 907.

13. G o r e l i k, L.L., R e d k o b o r o d y, J.N. and S i - n i t s y n, V.V., Soviet Phys. JETP **48** (1965) 761.

CHAPTER III

GENERAL DISCUSSION

3.1 Introduction

In the preceding chapters we described experiments on the in-
fluence of a magnetic field on the viscosity and the thermal con-
ductivity of polyatomic gases. It is the purpose of this chapter
to discuss these results in relation to the available theory. To
do this we will first give a survey of the experimental data and
of the main aspects of theory. In a subsequent section we compare
theory with the experimental results. It will be shown that to
explain the experimental results a theory has to take into account
the inelastic collisions.

Experimental data. In chapters I and II we compared the existing
data on viscosity and thermal conductivity with our results. For
reasons discussed there the older data on O_2 and NO appeared to
be unreliable in some aspects. We will not therefore include
these data when comparing with theory. G o r e l i k e.a.[1]
measured the influence of a magnetic field on the thermal conduc-
tivity of CO, N_2, H_2 and D_2. Their experiments were performed at
very low pressures (0.1 to 0.01 mm Hg) so that Knudsen effects
are of importance. In order to correct for these effects they
calibrated their apparatus by comparing the results obtained for
O_2 with the known values[2]. As we discussed in chapter II this
procedure seems rather doubtful. This is all the more true for
the H_2-isotopes as for these molecules the collision cross-section
for rotational-translational energy transfer is small. This im-
plies that the heat transfer by the internal degrees of freedom
is influenced by Knudsen effects at a much earlier stage than the
translational degrees of freedom[3]. In this sense the H_2-isotopes
behave differently from molecules like O_2 and N_2 where the cross-
section for energy conversion is far nearer to the elastic one.

In addition the accomodation coefficient for energy exchange at the wall is for the H_2-isotopes also different for rotational and translational energy[4]. These arguments are corroborated by the fact that the experimental curves for H_2 and D_2 do not start with $(H/p)^2$ as they ought to do (see fig. 3.1).
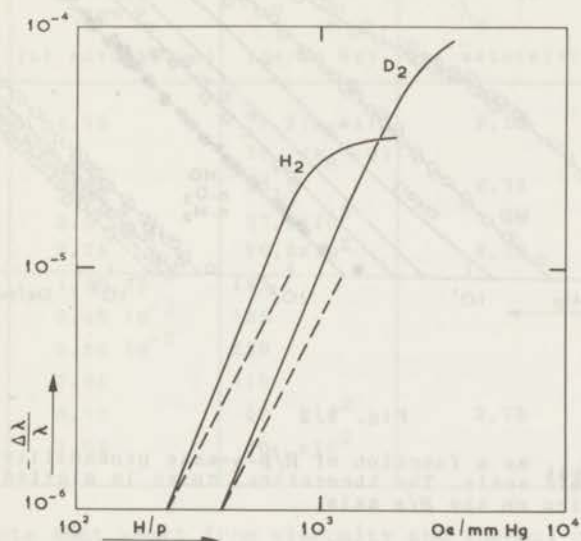
Fig. 3.1

The results of G o r e l i k   e. a.   for H_2 and D_2 as compared with theory (----) on a double logarithmic scale.

We exclude because of the unreliable calibration method the results for N_2 and CO of G o r e l i k e. a. Although according to the above mentioned reasons, these arguments are even stronger for the rejection of their results for H_2 and D_2, we will include them nevertheless in a qualitative discussion as they are the only existing thermal conductivity data.

In figs. 3.2 and 3.3 a survey is given of our results on the change of the viscosity and the thermal conductivity under the influence of a magnetic field. For simplicity of representation probability paper is used (see also chapter I). Table 3.I gives the two values characterizing each curve, i.e., the change in viscosity or thermal conductivity at saturation and the value of H/p where the effect reaches half the saturation value. For O_2

the $(H/p)_{1/2}$ values for the different magnetic states ($m_S = \pm 1$ and $m_S = 0$) are given.
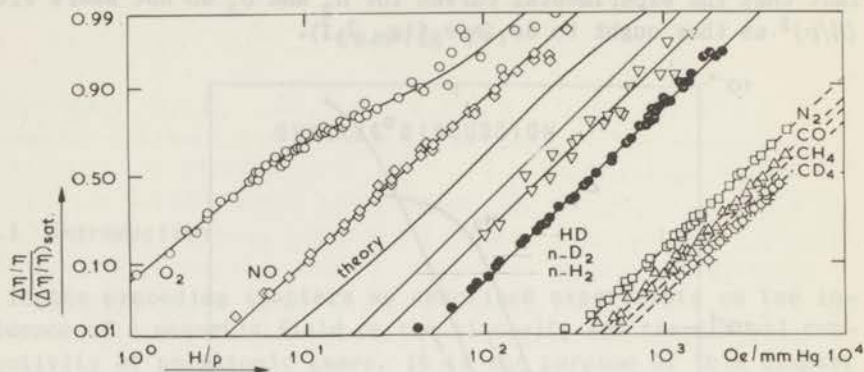
Fig. 3.2

$(\Delta\eta/\eta)/(\Delta\eta/\eta)_{sat}$ as a function of H/p. y-axis probability scale, x-axis logarithmic scale. The theoretical curve is plotted at an arbitrary position on the H/p axis.
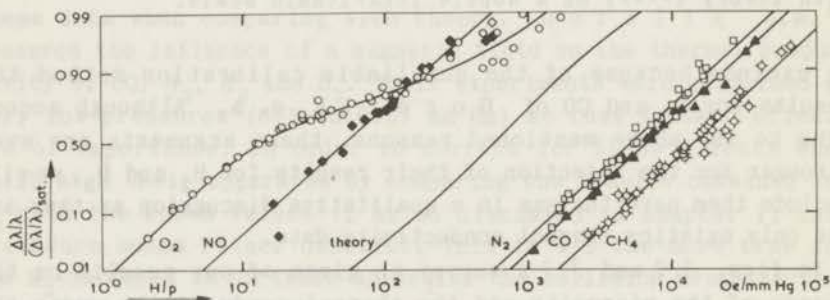
Fig. 3.3

$(\Delta\lambda/\lambda)/(\Delta\lambda/\lambda)_{sat}$ as a function of H/p. y-axis probability scale, x-axis logarithmic scale. The theoretical curve is plotted at an arbitrary position on the H/p axis.

54

Table 3.I

	viscosity		thermal conductivity	
	$\dfrac{\Delta\eta}{\eta_o}\,10^3$ (at saturation)	$(H/p)_{\frac{1}{2}}$ (Oe/mm Hg)	$\dfrac{\Delta\lambda}{\lambda_o}\,10^3$ (at saturation)	$(H/p)_{\frac{1}{2}}$ (Oe/mm Hg)
O_2	4.35	3.3 $(m_S=\pm1)$ 26 $(m_S=0)$	9.10	7.7 $(m_S=\pm1)$ 125 $(m_S=0)$
NO	2.77	33.5	6.75	33
N_2	3.0	27.5×10^2	7.90	53×10^2
CO	3.75	36.5×10^2	8.20	69×10^2
$n-H_2$	$1.60\ 10^{-2}$	145		
$p-H_2$	$3.45\ 10^{-2}$	125		
$n-D_2$	$3.50\ 10^{-2}$	220		
HD	1.94	410		
CH_4	0.77	42×10^2	2.75	157×10^2
CD_4	1.02	50×10^2		

We note that apart from viscosity and thermal conductivity experiments there are diffusion measurements by S e n f t l e b e n and S c h u l t[5]. They found a relative change of -2.10^{-4} in the diffusion coefficient for an $O_2 - H_2$ mixture. However, these results cannot be used in a more detailed comparison with theory.

There are also our measurements on transverse momentum transport which have a preliminary character[6] (see also appendix). As these data are qualitative as far as the magnitude of the effect is concerned we will not include them in the following discussion.

Theory. Explicit theoretical calculations with which quantitative comparison is meaningful are so far only performed for symmetric linear molecules treated along the lines of the Chapman and Enskog theory. In this theory the distribution function, in the presence of a small macroscopic gradient, is written as $f^o(1 + \chi)$, where f^o is the local equilibrium distribution and χ the deviation from equilibrium. In the presence of a temperature gradient, χ has the form

$$\chi = -\mathbf{A}. \, \nabla \ln T \tag{3.1}$$

55

and with a velocity gradient one has

$$\chi = -2\,B : (\text{Gråd }v) - C\,\text{div }v \tag{3.2}$$

where C gives rise to the volume viscosity which will not be considered here.

In a gas with rotational degrees of freedom the perturbed distribution function is anisotropic in both velocity, v, and rotational angular momentum, M, (see also refs. 7, 8 and 9). As a result A and B can be expanded in irreducible tensors made up of v and M. So one has e.g., for the thermal conductivity in the presence of a magnetic field H

$$A_i\,(v,M,H) = \sum_{p,q} A_{i\ k_1 \ldots\ k_{p+q}}^{p\ q}\,(H)\,[V_{k_1}\cdots V_{k_p}]\,[M_{k_{p+1}}\cdots M_{k_{p+q}}]$$

where the square brackets denote the irreducible tensors. The coefficients $A_{i\ k_1\ldots\ k_{p+q}}^{p\,q}\,(H)$ are functions of V^2, M^2 and H. This generalized expansion is necessary to take into account the mixing of directions caused by the precession of the molecular axis in the field. Applying the above method K a g a n and M a k s i m o v[10] calculated the change of the thermal conductivity of O_2 in a magnetic field. They limited their calculations to a simple elastic collision model in which a small non-sphericity of the molecule was included. No change of direction or magnitude of M upon collision was allowed. The rotational degrees of freedom of the molecules were treated classically. As a result of their collision model the only remaining term in A, on which the magnetic field acts, is of the $[v]\,[M\,M]$ type. In this way they give a more rigorous treatment of the original G o r t e r [11] – Z e r n i k e – V a n L i e r[12] mean free path picture. K n a a p and B e e n a k k e r[13] extended the work of K. M. to diamagnetic molecules. In their calculations they also treated the viscosity. Furthermore they included in their treatment explicitly the occurrence of transverse energy and momentum transport in a magnetic field. The K. M. elastic collision model is used throughout their work. As a consequence the only remaining term in B, containing M, is of the $[v\,v]\,[M\,M]$ type. The results of these calculations give the following expressions for the change of the viscosity and the thermal conductivity in a magnetic field.

56

For the relative change of the viscosity under our experimental conditions, i.e., averaged over the angles between gradients and field direction (see chapter I) one has

$$\frac{\Delta \eta}{\eta_0} = - \tilde{\psi} \left\{ \frac{13}{2} \frac{\tilde{\Theta}^2}{1+\tilde{\Theta}^2} + 5 \frac{4\tilde{\Theta}^2}{1+4\tilde{\Theta}^2} \right\} \tag{3.3}$$

and for the thermal conductivity (see chapter II)

$$\frac{\Delta \lambda}{\lambda_0} = \psi \left\{ \frac{3}{2} \frac{\Theta^2}{1+\Theta^2} + \frac{4\Theta^2}{1+4\Theta^2} \right\} \tag{3.4}$$

$\tilde{\psi}$ and ψ are directly related to the strength of the non-sphericity of the molecular interaction and contain furthermore the collision integrals Ω^{ls}, which are well known in elastic transport theory (see H. C. B.[14]). $\tilde{\Theta}$ and Θ are proportional to H/p and furthermore contain molecular constants and the earlier mentioned collision integrals.

Note that the expressions between brackets are only slightly different for viscosity and thermal conductivity.

3.2 Comparison of theory with experiment
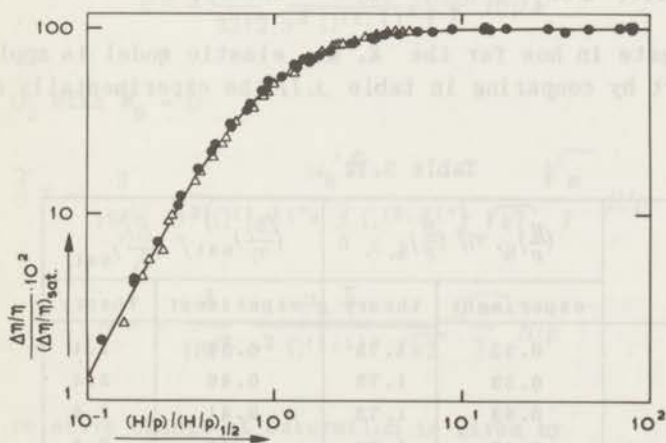
Fig. 3.4

$(\Delta\eta/\eta)/(\Delta\eta/\eta)_{sat}$ as a function of $(H/p)/(H/p)_{1/2}$ on a double logarithmic scale. ● NO; △ HD; ——theory.

In figs. *3.2* and *3.3* the curves corresponding to the theoretical expressions *(3.3)* and *(3.4)* are drawn. As one can see they become nearly straight lines in this representation. Agreement with experiment is excellent. This is further illustrated in figs. *3.4* and *3.5*.
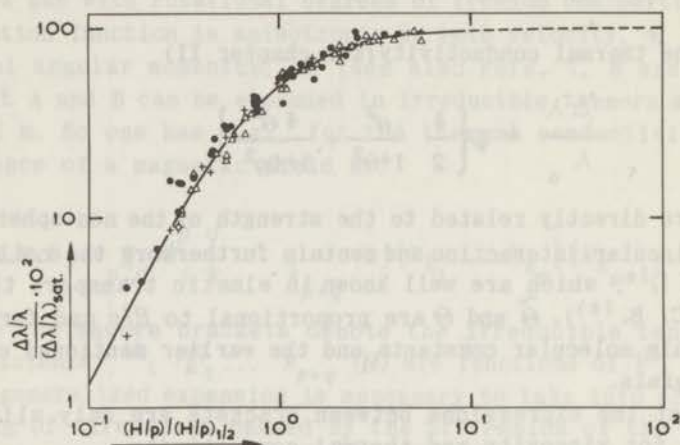
Fig. 3.5

$(\Delta\lambda/\lambda)/(\Delta\lambda/\lambda)_{sat}$ as a function of $(H/p)/(H/p)_{\frac{1}{2}}$ on a double logarithmic scale. ● CH$_4$; △ N$_2$; + CO; ——theory.

To investigate in how far the K. M. elastic model is applicable we start by comparing in table *3.II* the experimentally and

Table 3.II

	$(\frac{H}{p})_{\frac{1}{2}}$, $\eta/(\frac{H}{p})_{\frac{1}{2}}$, λ		$(\frac{\Delta\eta}{\eta})_{sat}/(\frac{\Delta\lambda}{\lambda})_{sat}$	
	experiment	theory	experiment	theory
N$_2$	0.52	1.73	0.38	2.4
CO	0.53	1.73	0.46	2.4
NO	0.63	1.73	0.41	2.4
O$_2$ ($m_S=\pm 1$)	0.43	1.73	0.48	2.4
O$_2$ ($m_S = 0$)	0.21	1.73	0.48	2.4
CH$_4$	0.27		0.28	

theoretically obtained ratio between the $(H/p)_{1/2}$ values for viscosity and thermal conductivity. The same is done for the relative changes at saturation. Taking ratios we avoid complications arising from uncertainties in non-sphericity parameters and magnetic moments and compare directly the qualitative features of the theory. For $\tilde{\Theta}$ and Θ, which describe the field dependence in eqs. (3.3) and (3.4), the following expressions are used[10] [13]. For diamagnetic molecules

$$\tilde{\Theta} = \frac{3}{8\sqrt{\pi}} \frac{g\,\mu_N\,\sqrt{kTm}}{\hbar\sigma^2\left\{\Omega^{(1,1)*} + \frac{3}{5}\,\Omega^{(2,2)*}\right\}}\,H/p \tag{3.5}$$

$$\Theta = \frac{3}{8\sqrt{\pi}} \frac{g\,\mu_N\,\sqrt{kTm}}{\hbar\sigma^2\,\Omega^{(1,1)*}}\,H/p \tag{3.6}$$

For O_2 with $m_S = \pm 1$

$$\tilde{\theta} = -\frac{9}{32\sqrt{2}} \frac{\mu_B\,m_S}{\sigma^2\left\{\Omega^{(1,1)*} + \frac{3}{5}\,\Omega^{(2,2)}\right\}}\sqrt{\frac{m}{I}}\,H/p \tag{3.7}$$

$$\theta = -\frac{9}{32\sqrt{2}} \frac{\mu_B\,m_S}{\sigma^2\,\Omega^{(1,1)*}}\sqrt{\frac{m}{I}}\,H/p \tag{3.8}$$

For O_2 with $m_S = 0$

$$\tilde{\tilde{\theta}} = -\frac{3}{16\sqrt{\pi}} \frac{\mu_B\,\hbar}{\sigma^2\left\{\Omega^{(1,1)*} + \frac{3}{5}\,\Omega^{(2,2)*}\right\}\sqrt{kT}} \frac{\sqrt{m}}{I}\,H/p \tag{3.9}$$

$$\tilde{\theta} = -\frac{3}{16\sqrt{\pi}} \frac{\mu_B\,\hbar}{\sigma^2\,\Omega^{(1,1)*}\,\sqrt{kT}} \frac{\sqrt{m}}{I}\,H/p \tag{3.10}$$

the relative change at saturation is given by

$$\frac{\Delta\eta}{\eta_0} = -\frac{69}{4900}\,\beta^2\,\frac{\Omega^{22}}{\Omega^{11} + \frac{3}{10}\,\Omega^{22}} \tag{3.11}$$

59

$$\frac{\Delta\lambda}{\lambda_o} = -\frac{3}{25}\beta^2 \; (1-\frac{3}{4}\frac{\Omega^{21}}{\Omega^{11}})^2 \; \{1+\frac{25}{4}\frac{\Omega^{11}}{\Omega^{22}} \; [1-\frac{4}{25}\beta^2(1-\frac{3}{4}\frac{\Omega^{21}}{\Omega^{11}})^2]\}^{-1} \qquad (3.12)$$

Hence, for the ratio of $(H/p)_{1/2}$ for viscosity and thermal conductivity one has

$$\frac{(H/p)_{1/2,\eta}}{(H/p)_{1/2,\lambda}} = \frac{\widetilde{\Theta}_{1/2}}{\Theta_{1/2}} \; (1+\frac{3}{5}\frac{\Omega^{(2,2)*}}{\Omega^{(1,1)*}}) \qquad (3.13)$$

with $\widetilde{\Theta}_{1/2} = 0.742$ and $\Theta_{1/2} = 0.762$ as obtained from (3.3) and (3.4). For $(\Delta\eta/\eta_o)_{sat}/(\Delta\lambda/\lambda_o)_{sat}$ one obtains

$$\frac{(\Delta\eta/\eta_o)_{sat}}{(\Delta\lambda/\lambda_o)_{sat}} = \frac{115}{294} \; \frac{(1+\frac{25}{4}\frac{\Omega^{11}}{\Omega^{22}})}{(1+\frac{10}{3}\frac{\Omega^{11}}{\Omega^{22}})(1-\frac{3}{4}\frac{\Omega^{21}}{\Omega^{11}})^2} \qquad (3.14)$$

where in expression (3.14) terms in β^2 are neglected as they are very small.

The symbols used are: μ_N nuclear magneton, μ_B Bohr magneton, k Boltzmann's constant, $\hbar$ Planck's constant, T temperature; the molecular constants m mass, I moment of inertia, σ diameter, g rotational Landé's g-factor and the parameter β characterizing the non-sphericity of the molecular interaction. For the definition of Ω^{ls} and $\Omega^{(l,s)*}$ see H. C. B. [14].

Closed-form expressions for the collision integrals are available for the hard sphere model. For a Lennard-Jones potential $\Omega^{(l,s)*}$ is tabulated with the exception of $\Omega^{(2,1)*}$. The integrals Ω^{ls} are proportional to σ^2 and are a function of kT/ϵ where σ and ϵ are the potential parameters. The expressions (3.13) and (3.14) contain only ratios of Ω^{ls}, hence they do not depend on σ but only on kT/ϵ. As far as the tabulated quantities are concerned we know that their ratios are practically independent of ϵ and not too different from the corresponding values for hard spheres. There is no reason why Ω^{21} will behave differently from the other integrals. So we used in (3.14) the hard sphere value for the ratio containing Ω^{21}. We expect that the ratio $\Omega^{(2,1)*}/\Omega^{(1,1)*}$ will

not deviate more than 20% from unity. This would cause a corresponding variation of 40% in $(\Delta\eta/\eta_o)_{sat}/(\Delta\lambda/\lambda_o)_{sat}$.

It is clear from table $3.II$ that the elastic approximation does not work. Even the uncertainty introduced by lack of knowledge of exact numerical values of Ω^{21} can never account for the observed difference. The discrepancy not only exists in the ratios but both in viscosity and thermal conductivity. This can be seen by comparing $(H/p)_{1/2}$ values from theory with experiment. The comparison is made with this quantity as all parameters in eqs. (3.5) to (3.10) are known. This is in contrast with the change at saturation which depends on the rather uncertain value of the non–sphericity parameter β. In table $3.III$ the ratio of $(H/p)_{1/2}$ for

Table 3.III

	g	viscosity $\dfrac{(H/p)_{1/2},\text{th}}{(H/p)_{1/2},\text{exp}}$	thermal conductivity $\dfrac{(H/p)_{1/2},\text{th}}{(H/p)_{1/2},\text{exp}}$
O_2 ($m_S = \pm 1$)	15)	1.89	0.51
O_2 ($m_S = 0$)	15)	3.78	0.49
N_2	0.28 16)	1.98	0.63
CO	0.27 17)	1.54	0.51
$p-H_2$	0.88 18)	26.9	
$n-H_2$	0.88 18,19)	23.2	(≈ 1)
$n-D_2$	0.44 18)	21.5	(≈ 1)
HD	0.66 20,	8.9	

The data between brackets are taken from the work of G o r e - l i k e. a.[1].

theory and experiment is given for the viscosity and the thermal conductivity. The rotational Landé's g-factors used were taken from refs. 15, 16, 17, 18, 19 and 20. The g value for N_2 has been estimated from the value for $^{15}N_2$ (see e.g. ref. 21). We see that both in viscosity and thermal conductivity the ratio is not unity as should be expected. The directions of the deviations are even different for both phenomena. From table $3.II$ we see that the experimental value of $(H/p)_{1/2,\eta}$ is always smaller than $(H/p)_{1/2,\lambda}$,

while $(H/p)_{\frac{1}{2},\lambda}$ corresponds roughly to the time between two elastic collisions (see table $3.III$). The elastic theory, however, gives $(H/p)_{\frac{1}{2},\eta} > (H/p)_{\frac{1}{2},\lambda}$, which is directly related to the existence of an Eucken factor > 1. This means that improvements within an elastic collision model will not give the desired result and as such inelastic collisions have to be included.

At this point we will introduce the work of M c C o u r t and S n i d e r[22]. They give a formal treatment of the magnetic effect on the thermal conductivity for linear molecules with interactions of which the non-sphericity can be treated as a perturbation. The rotational degrees of freedom are treated quantum mechanically. Their treatment is also valid for models with inelastic collisions, i.e., for the case that M changes upon collision. The calculations have been performed for the same type of anisotropy in the distribution function, $[v][MM]$, that was used in the calculations of K. M.. Another possible simple type of anisotropy, $[v][M]$, that does not exist for the K.M. model has been explicitly neglected. The results of this theory are expressed in terms of collision integrals that contain elastic and inelastic collision cross-sections. These integrals can only be numerically evaluated after a further specification of a collision model. This means that the theory as such gives only qualitative information. Their solution of the Boltzmann equation is formally identical to that of K. M. and K. B.. So apart from scale factors (i.e., different values for the collision integrals) their results for the field dependence of the thermal conductivity is identical to that obtained by K. M. and K. B.. The same will be true for the viscosity provided that the calculations are limited to the same type of anisotropy used in the elastic treatment.

In general one can say that in a field every type of anisotropy in the distribution function, containing M, may give rise to a change of the transport coefficients. The field dependence will show a dispersion type behaviour. Apart from scale factors the curve is independent of the collision process as long as the calculations are limited to a model with small non-sphericity. The collision process determines the magnitude of the effect and the characteristic time occurring in the dispersion expression, i.e., the position of the curve on the H/p axis. Each type of anisotropy has in general its own characteristic time, τ. Thus if more than one type of anisotropy can contribute to the field effect one will

62

deal with a curve which is the result of contributions associated with the different values of τ. It is clear that it is very difficult to distinguish directly between the various contributions unless the τ's present are separated far enough. So one has to be very careful in drawing conclusions from the universal shape of the approach to saturation in figs. 3.4 and 3.5. This agrees with the fact that CH_4 and CD_4 also follow the same curve as the linear molecules.

To judge the consequences of this situation we will first consider the times associated with the collision processes that can occur. In simple diatomic gases at room temperature one has to distinguish only the following types of collisions: elastic collisions ($\triangle m_J = 0$, $\triangle J = 0$; J and m_J are the quantum numbers characterizing the rotational state of the molecule), inelastic collisions at which the orientation of the molecular axis changes but not the internal energy ($\triangle m_J \neq 0$, $\triangle J = 0$) and collisions at which also the internal energy changes ($\triangle m_J \neq 0$, $\triangle J \neq 0$). From acoustical relaxation measurements[23] [24] one knows that for the heavier molecules like N_2 the Maxwellian average of the cross-section for translational-rotational energy exchange, $\sigma_{\triangle J}$, is about one tenth of the elastic cross-section, σ_{el}. Transitions at which only $\triangle m_J \neq 0$ will be more frequent than the energetically inelastic collisions. So the different cross-sections are not widely separated and their contributions will tend to overlap. Therefore it will be difficult to distinguish directly between the contributions of different types of collisions. The H_2-isotopes, however, offer better possibilities. From N.M.R.[25] [26] and acoustical relaxation[27] [28] experiments one knows that for the homonuclear molecules H_2 and D_2 at room temperature the three collision cross-sections are far more apart. For H_2 at room temperature e.g., one has as far as orders of magnitude are concerned $\sigma_{el} : \sigma_{\triangle m_J} : \sigma_{\triangle J} \approx 100 : 10 : 1$. One may expect in this case a clear separation of the different collision processes. For heteronuclear HD $\sigma_{\triangle J}$ is strongly influenced by the fact that in a heteronuclear molecule the transition $\triangle J = \pm 1$ becomes possible (in H_2 only $\triangle J = \pm 2$ exists). Further the effective non-sphericity is increased by the asymmetric mass distribution. As a result $\sigma_{el} : \sigma_{\triangle J}$ is of the order of 10. We will see later that there are indications that $\sigma_{\triangle m_J} \approx \sigma_{\triangle J}$.

From table $3.III$ we see that the values of $(H/p)_{\frac{1}{2}, \eta}$ and $(H/p)_{\frac{1}{2}, \lambda}$ for H_2 and D_2 are widely separated and correspond to a characte-

ristic time associated with $\sigma_{\Delta m_J}$ and σ_{e1} respectively. The viscosity measurements of H_2 and D_2 do not exclude a possible contribution of elastic collisions, because our measurements were not extended to H/p values corresponding to the time scale of elastic collisions. Combining, however, the results for the H_2-isotopes with the information obtained for the heavier molecules where always $(H/p)_{\frac{1}{2},\eta} < (H/p)_{\frac{1}{2},\lambda}$, we come to the conclusion that for the magnetic effect in the viscosity inelastic collisions and in the thermal conductivity elastic collisions are dominant. We are inclined to extrapolate this to the field free case, i.e., the type of anisotropy in M that is of importance for the viscosity is mainly related to inelastic collisions while the opposite is true for the thermal conductivity. In this picture the behaviour of HD can be understood if we assume that $\sigma_{\Delta m_J} \approx \sigma_{\Delta J}$.

Using the rough spherical model C o n d i f f, W e i – K a o and D a h l e r [29] considered recently in the field free case the relative importance of the different terms anisotropic in M that occur in the expansion of *(3.1)* and *(3.2)*. Their conclusion is, that for the thermal conductivity the term [V] [M M] and for the viscosity the term [M M] give the dominant contribution. The first term is sensitive to elastic collisions through the angle between V and M, but the last one to inelastic collisions only. Furthermore one can easily show that a term in B of the form *constant* x [M M] gives no contribution to the viscosity in an elastic collision model. This would explain the different behaviour of viscosity and thermal conductivity in a magnetic field as found experimentally. Recently, however, M c C o u r t [30] proved that for any well behaved collision model the contribution of [M M] alone will vanish also in the inelastic case. So the results of C o n d i f f e. a. are presumably due to the pathology of the rough spherical model or to the fact that their expansion of B in V and M is not irreducible. Anyhow the situation remains still open and a further theoretical analysis that includes also other terms in the expansion of B is needed.

We will now make some remarks on the behaviour of O_2 and on the difference between normal and para H_2. The behaviour of O_2 can be explained with the help of the foregoing ideas. In trying to separate the contribution to the effect of the $m_S = \pm 1$ states from those of the state with $m_S = 0$ we arrive at the data given in table *3.I*. To obtain these results we assume that the contributions of the different magnetic states are superimposed and that

individually they behave very similar to the other gases as a function of H/p. While the contributions of the different m_S states appear to be roughly equal, the ratio of $(H/p)_{\frac{1}{2}}$ between the $m_S = \pm 1$ states and the $m_S = 0$ state for the thermal conductivity differs from that for the viscosity. In the thermal conductivity the ratio is what one would expect for the elastic model in which the cross-sections do not depend on m_S. This is, however, not the case for the viscosity (see table $3.IV$). This suggests that $\sigma_{\Delta m_J}$ depends on m_S, i.e., on the orientation of the electron spin with respect to the molecular axis, which is not unreasonable.

Table 3.IV

	experiment		elastic theory	
	η	λ	η	λ
$\dfrac{(H/p)_{\frac{1}{2}},\ m_S = 0}{(H/p)_{\frac{1}{2}},\ m_S = \pm 1}$	7.9	16.2	15.7	15.7

In chapter I we showed that the difference in the magnetic effect for the viscosity between normal and para H_2 points to the fact that both in magnitude and $(H/p)_{\frac{1}{2}}$ value, the behaviour of normal H_2 is dominated by para H_2 with $J = 2$. This can be explained in the following way. It is well known that $\sigma_{\Delta m_J}$ depends strongly on the anisotropy in the long-range forces as opposed to the situation for $\sigma_{\Delta J}$. For the H_2-isotopes the anisotropy in the long-range forces depends on the rotational state and is larger for $J = 2$ than for $J = 1$. (cf. B l o o m and O p p e n h e i m [31]). Thus in normal H_2 the para H_2 molecules in $J = 2$ will give the dominant contribution to the magnetic effect. It is interesting to see how this type of experiments, as also N.M.R., can give information complementary to that obtained from acoustical work. The magnetic effect on the transport properties makes it possible, unlike N.M.R., to investigate also para H_2 (with total nuclear spin zero).

We will end this chapter with some suggestions for experimental work that might further clarify the situation.

a It is evident that experimental work on the H_2-isotopes is most promising. More accurate experiments on the thermal conduc-

tivity are needed. To decide on the importance of the elastic collisions in the viscosity, experiments are needed at the same (H/p) values at which the effect occurs for the thermal conductivity. Furthermore it will be interesting to study the temperature dependence of the effect in η and compare these results with what is known of the temperature dependence of the inelastic collisions from N.M.R. measurements[25) 32)]. In the same line are to be mentioned experiments on mixtures with noble gases for which N.M.R. results are available[26) 33)].

b To decide the importance of the $[\mathbf{v}][\mathbf{M}]$ term in the thermal conductivity it will be interesting to study the difference between $(\Delta\lambda/\lambda_o)_\perp$ and $(\Delta\lambda/\lambda_o)_\parallel$. The reason is that this term as shown by M c. S. does not contribute if the field is perpendicular to the temperature gradient.

TRANSVERSE MOMENTUM TRANSPORT IN VISCOUS FLOW

We will present here the results of our work on the transverse momentum transport in viscous flow of diatomic gases in a magnetic field. In view of the preliminary character of this work and of the fact that experiments are still in progress we limit ourselves here to the presentation of a note on this subject as published in Physics Letters 21 (1966) 1[6]. We like to thank the North Holland Publishing Cy. for their kind permission.

Recently, as a result of the generalization of the Senftleben-effect[34], experimental work has been published about the change in the viscosity and the thermal conductivity of polyatomic molecules in a magnetic field[1][35][36][37], for a survey see ref. 36.
According to a phenomenological treatment of the viscosity and the thermal conductivity of a fluid in a magnetic field given by H o o y m a n e. a.[38][39], transverse phenomena similar to the Hall-effect in electrical conductivity may also occur here. Till now transverse heat transfer was only experimentally found for some solids where it is known as the Righi–Leduc effect[40][41]. A theoretical analysis[13] by extending the work of K a g a n[10] showed that in the case of diatomic gases in a magnetic field these effects indeed exist in the viscosity and the thermal conductivity (see also W a l d m a n n[42]).
It is the purpose of this note to report experimental results of the transverse effect in the case of viscosity for O_2, N_2 and HD at room temperature.

67

The situation for viscous flow in a magnetic field is described
by means of a scheme of coefficients that connect the symmetric
pressure tensor with the symmetric velocity gradient tensor. The
part of the scheme which is relevant for our measurements is
given by (H is chosen as the x-axis)

	$(\text{Gr\mathring{a}d } v)^s_{yz}$	$(\text{Gr\mathring{a}d } v)^s_{zx}$	$(\text{Gr\mathring{a}d } v)^s_{xy}$
$\overset{os}{\Pi}_{yz}$	$-2(2\eta_2-\eta_1)$	0	0
$\overset{os}{\Pi}_{zx}$	0	$-2\eta_3$	$-2\eta_5$
$\overset{os}{\Pi}_{xy}$	0	$+2\eta_5$	$-2\eta_3$

$$(3.15)$$

It follows from spatial symmetry that in the absence of a magnetic
field, the diagonal elements are equal to $\eta_{H=0}$, while the off-
diagonal elements vanish. In the presence of a magnetic field the
diagonal elements in this scheme are, for symmetry reasons, even
and the off-diagonal ones are odd in H.

In order to measure η_5 we made a long flat tube with $d \ll b$ and
l (see fig. 3.6), so that the flow pattern in the tube is mainly
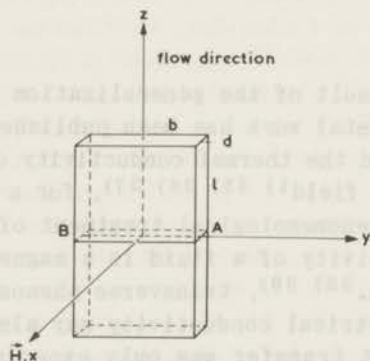
Fig. 3.6

Schematic diagram of the experimental set-up.

determined by $\partial v_z/\partial x$. In the absence of a magnetic field $\partial v_z/\partial x$
(i.e. $(\text{Gr\mathring{a}d } v)^s_{zx}$) is only connected to $\overset{os}{\Pi}_{zx}$. However, in a magne-
tic field there is also a connection between $\partial v_z/\partial x$ and $\overset{os}{\Pi}_{xy}$ by
the coefficient η_5. This leads to pressure difference in the y-

direction which is measured with a differential manometer between A and B. In a first approximation η_5 can be calculated from

$$\eta_5/\eta_0 = (p_A - p_B)/b(\partial p/\partial z)_{AB} \qquad (3.16)$$

We measured the effect for O_2, N_2 and HD (see figs. 3.7 and 3.8). The observed pressure difference changes sign if the direction of the field is reversed. For convenience the effect is plotted for one field direction.

Qualitatively the experiments are in fair agreement with results of theoretical calculations[13]. These give for η_5 the following relation:

$$\frac{\eta_5}{\eta_0} = \tilde{\psi} \left\{ 5 \frac{\tilde{\Theta}}{1 + \tilde{\Theta}^2} - 6 \frac{2\tilde{\Theta}}{1 + 4\tilde{\Theta}^2} \right\} \qquad (3.17)$$

wherein $\tilde{\Theta} = K \mu H/p$, μ is the magnetic moment of the molecule and p is the pressure of the gas. The constants $\tilde{\psi}$ and K are functions of the molecular constants and the collision integrals Ω^{ls}. The formula predicts that η_5 changes sign at some value of H/p. This was indeed found in the case of O_2. We could measure only part of the curve of N_2 and HD under our experimental conditions ($H_{max} = 20.000$ Oe and $p_{min} = 5$ mm Hg) because the magnetic moments of N_2 and HD are much smaller than that of O_2.

As η_5 is an odd function of μ, its sign will depend on that of μ or on that of the rotational Landé factor g_J. The sign of the observed effect for HD is consistent with the known positive value of g_J[15)20)]. In the case of O_2 the situation is slightly more complicated as the magnetic moment arises from the $^3\Sigma$ state of the molecule (for a discussion of the magnetic moment of O_2 see ref. 15). In this state the electron spin angular momentum $S = 1$ which is coupled to the rotational axis of the molecule can have three orientations with respect to this axis: $m_S = \pm 1, 0$. The contributions of the $m_S = +1$ and $m_S = -1$ states to η_5 cancel. Only the third of the molecules with $m_S = 0$, that have a small magnetic moment anti-parallel to the total angular momentum, contributes to the transverse effect (for details see chapter I and ref. 13). This is in agreement with the observed sign of η_5 and with the fact that η_5 is much smaller for O_2 than for N_2. Since in the case of N_2 the observed effect has the same direction as
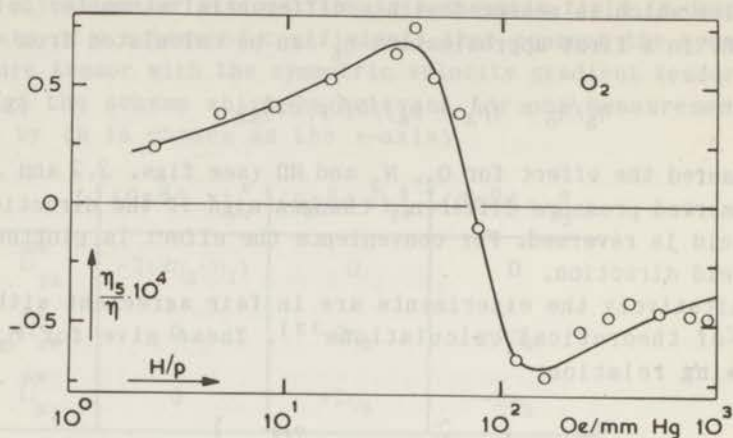
Fig. 3.7

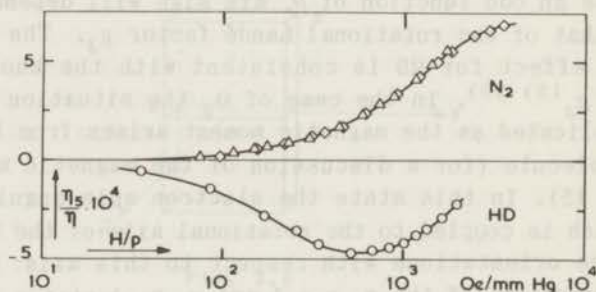η_5/η_0 as a function of H/p for O_2; $p = 20.40$ mm Hg.

Fig. 3.8

η_5/η_0 as a function of H/p for N_2 and HD.

N_2 ◇ 5.26 mm Hg   HD ○ 9.52 mm Hg

N_2 △ 10.73 mm Hg

for O_2, one can conclude to a negative g_J for N_2. Thus this type of measurements enables one to determine the sign of g_J of the molecular magnetic moments. This is of importance since in most cases the magnetic resonance measurements give only its absolute value[16].

Full details of measurements on CO, CO_2 and molecules like CH_4 etc. will appear in Physica. Preliminary measurements of the transverse effect in the thermal conductivity have also been carried out[43].

REFERENCES

1. G o r e l i k, L.L., R e d k o b o r o d y, J.N. and S i-
   n i t s y n, V.V., Soviet Phys. JETP **48** (1965) 761.
2. S e n f t l e b e n, H. and P i e t z n e r, J., Ann. Phys.
   16 (1933) 907.
3. W a e l b r o e c k, F.G. and Z u c k e r b r o d t, P.,
   J. chem. Phys. **28** (1958) 524.
4. S c h ä f e r, K. and S t o t z, S., Z. Elektrochem., Ber.
   Bunsenges. physik. Chem. **65** (1961) 623.
5. S e n f t l e b e n, H. and S c h u l t, H., Ann. Phys. **7** (1950)
   103.
6. K o r v i n g, J., H u l s m a n, H., K n a a p, H.F.P. and
   B e e n a k k e r, J.J.M., Phys. Letters **21** (1966) 1.
7. W a l d m a n n, L., Z. Naturforschung **12a** (1957) 660.
8. W a l d m a n n, L. and T r ü b e n b a c h e r, E., Z. Na-
   turforschung **17a** (1962) 363.
9. K a g a n, Y. and A f a n a s e v, A.M., Soviet Phys. JETP
   14 (1962) 604.
10. K a g a n, Y. and M a k s i m o v, L.L., Soviet Phys. JETP
    14 (1962) 1096.
11. G o r t e r, C.J., Naturwiss. **26** (1938) 140.
12. Z e r n i k e, F. and V a n L i e r, C., Physica **6** (1939)
    961.
13. K n a a p, H.F.P. and B e e n a k k e r, J.J.M., Commun. Ka-
    merlingh Onnes Lab. Leiden, Suppl. No. **124**; Physica **32** (1966).

14. H i r s c h f e l d e r, J.O., C u r t i s, C.F. and B y r o n B i r d, R.B., Molecular theory of Gases (John Wiley and Sons, New York, 1954).

15. H e r z b e r g, G., Molecular Spectra and Molecular Structure (D. VanNostrand Cy. Inc., Princeton, New Yersey, 1961).

16. C h a n, S.I., B a k e r, M.R. and R a m s e y, N.F., Phys. Rev. 136 (1964) A 1224.

17. R o s e n b l u m, B.A., N e t h e r c o t, A.H. and T o w n e s, C.H., Phys. Rev. 169 (1958) 400.

18. H a r r i c k, N.J., B a r n e s, R.G., B r a y, P.J. and R a m s e y, N.F., Phys. Rev. 90 (1953) 260.

19. H a r r i c k, N.J. and R a m s e y, N.F., Phys. Rev. 88 (1952) 228.

20. Q u i n n, W.E., B a k e r, J.M., La T o u r e t t e, J.T. and R a m s e y, N.F., Phys. Rev. 112 (1958) 1929.

21. B r o o k s, R.A., A n d e r s o n, C.H. and R a m s e y, N.F., Phys. Rev. Letters 10 (1963) 441.

22. M c C o u r t, F.R., Thesis, University of British Columbia, Canada 1966.

23. H e r z f e l d, K.F. and L i t o v i t z, Th.A., Absorption and Dispersion of ultrasonic-Waves (Academic Press Inc., New York and London, 1965) p. 239.

24. B a u e r, H.J. and K o s c h e, H., Acustica 17 (1966) 96.

25. L i p s i c a s, M. and B l o o m, M., Can. J. Phys. 39 (1961) 881.

26. J o h n s o n Jr., C.S. and W a u g h, J.S., J. chem. Phys. 36 (1962) 2266.

27. S l u y t e r, C.G., K n a a p, H.F.P. and B e e n a k k e r, J.J.M., Physica 30 (1964) 745.

28. S l u y t e r, C.G., K n a a p, H.F.P. and B e e n a k k e r, J.J.M., Physica 31 (1965) 915.

29. C o n d i f f, D.W., W e i - K a o L u and D a h l e r, J.S., J. chem. Phys. 42 (1965) 3445.

30. M c C o u r t, F.R. (private communication).

31. B l o o m, M. and O p p e n h e i m, I., Can. J. Phys. 41 (1963) 1580.

32. L i p s i c a s, M. and H a r t l a n d, A., Phys. Rev. 131 (1963) 1187.

33. W i l l i a m s, D.L., Can. J. Phys. 40 (1962) 1027.

34. B e e n a k k e r, J.J.M., S c o l e s, G., K n a a p, H.F.P. and J o n k m a n, R.M., Phys. Letters 2 (1962) 5.

72

35. G o r e l i k, L.L. and S i n i t s y n, V.V. Soviet Phys.
    JETF **19** (1964) 272.
36. B e e n a k k e r, J.J.M., H u l s m a n, H., K n a a p,
    H.F.P., K o r v i n g, J. and S c o l e s, G., Advances in
    thermophysical properties at extreme temperatures and pres-
    sures, ed. S. Gratch, (ASME, Purdue University, Lafayette,
    Indiana, 1965) p. 216.
37. K o r v i n g, J., H u l s m a n, H., K n a a p, H.F.P. and
    B e e n a k k e r, J.J.M., Phys. Letters **17** (1965) 33.
38. H o o y m a n, G.J., M a z u r, P. and D e G r o o t, S.R.,
    Physica **21** (1955) 355.
39. D e G r o o t, S.R. and M a z u r, P., Non–equilibrium
    thermodynamics, (North–Holland Publishing Cy., Amsterdam,
    1962) p. 311.
40. R i g h i, A. Atti Accad. Lincei **3** (1) (1887) 481.
41. L e d u c, A., J. Phys. **6** (1887) 373.
42. W a l d m a n n, L. and K u p a t t, H.D., Z. Naturforschung
    18a (1963) 86.
43. K o r v i n g, J., H u l s m a n, H., H e r m a n s, L.J.F.,
    D e G r o o t, J.J., K n a a p, H.F.P. and B e e n a k –
    k e r, J.J.M., J. Mol. Spec. **20** (1966) 294.

SAMENVATTING

Tot voor kort was het niet wel mogelijk een uitspraak te doen
omtrent de waarde van theoretische berekeningen over de transport-
coëfficiënten van gassen van meer-atomige moleculen. Afgezien van
een voor de hand liggende bijdrage van de rotatie energie tot de
warmtegeleiding – tot uitdrukking gebracht door de Eucken-factor
– vormen, bij eenvoudige moleculen, de bijdragen tot de transport-
coëfficiënten afkomstig van het niet-bolvormige deel van het in-
termoleculaire krachtveld, slechts een geringe correctie op het
dominerende spherisch-symmetrische deel. De recente ontdekking
dat de viscositeit en de warmtegeleiding van meer-atomige mole-
culen beïnvloed worden door een magnetisch veld opent de moge-
lijkheid bijdragen van de niet-bolvormigheid direct te bepalen.
Dit kan als volgt worden ingezien. Door W a l d m a n n en
K a g a n werd erop gewezen dat in de aanwezigheid van een gra-
diënt van een macroscopische grootheid (b.v. van de temperatuur)
de verdelingsfunctie anisotroop wordt in snelheden en impuls-
momenten beide. Dit in tegenstelling tot de eerder gebruikelijke
bewering dat de verdelingsfunctie nog wel isotroop blijft in de
impulsmomenten. In een magnetisch veld zal het magnetisch moment
van het molecuul, en daarmee de rotatie-as, een precessie gaan
uitvoeren om de veldrichting. Ten gevolge van deze precessie
wordt de anisotropie in de verdeling der impulsmomenten beïnvloed
en ten gevolge hiervan ook de transport-coëfficiënten. Daar de
anisotropie in de impulsmomenten zijn oorsprong vindt in het niet-
bolvormig zijn van de moleculaire wisselwerking, zal de invloed
van het magnetisch veld op de transport-coëfficiënten dus recht-
streeks verband houden met de bijdrage tot deze grootheden afkom-
stig van het niet-bolvormige deel der interactie.

De verandering van de viscositeit onder invloed van een magne-
tisch veld werd gemeten voor O_2, NO, N_2, CO, CO_2, CH_4, CD_4, CF_4, H_2, D_2
en HD; de verandering van de warmtegeleiding werd bepaald voor O_2,
NO, N_2, CO en CH_4. Alle metingen werden verricht bij kamertempera-
tuur. Een overzicht van de gebruikte meetmethoden wordt gegeven in
de hoofdstukken I en II. In hoofdstuk III volgt een vergelijking

van de experimentele resultaten met de theorie. Theoretische bere-
keningen van het magnetisch effect, voor een elastisch botsingsmo-
del met een geringe niet-bolvormigheid, zijn ontwikkeld door K a-
g a n en M a k s i m o v en later uitgebreid en verdiept door
K n a a p en B e e n a k k e r. De laatsten geven onder meer
een expliciete uitdrukking voor transversaal energie- en impuls-
transport in een magnetisch veld. Een beschrijving van experi-
menten hierover wordt gegeven in een appendix.

Het blijkt dat een theorie welke slechts elastische botsingen be-
schouwd, niet in staat is om een volledige verklaring te geven van
de experimentele resultaten. De resultaten van de viscositeits-
metingen duiden erop dat inelastische botsingen een belangrijke
rol spelen.

Teneinde te voldoen aan het verzoek van de Faculteit der Wiskunde en Natuurwetenschappen volgt hier een overzicht van mijn studie.

Na het afleggen van het H.B.S.–B examen in 1954 aan de 1° Christelijke H.B.S. te 's-Gravenhage, begon ik mijn studie in de natuurkunde aan de Rijksuniversiteit te Leiden. In 1959 legde ik het candidaatsexamen in de natuur- en wiskunde met bijvak sterrekunde af. Vervolgens vervulde ik mijn militaire dienstplicht als reserve officier bij de Koninklijke Landmacht. In 1961 hervatte ik mijn studie in de natuurkunde. Mijn practische opleiding genoot ik in het Kamerlingh Onnes Laboratorium in de werkgroep voor molecuulphysica. De leiding van deze groep berustte aanvankelijk bij Prof. Dr. K.W. T a c o n i s en is sedert 1963 in handen van Prof.Dr. J.J.M. B e e n a k k e r. Tot begin 1962 assisteerde ik Dr. H.F.P. K n a a p bij metingen van de mengwarmte van de waterstof-isotopen in de vloeistoffase. Na de vereiste tentamens te hebben afgelegd bij Prof. Dr. P. M a z u r, Prof.Dr. S.R. de G r o o t en Prof.Dr. J.A.M. C o x deed ik in november 1963 het doctoraal examen experimentele natuurkunde. Sindsdien ben ik als wetenschappelijk medewerker in dienst van de Stichting voor Fundamenteel Onderzoek der Materie. Vanaf 1962 heb ik geassisteerd op het practicum voor praecandidaten.

In 1965 was ik een maand werkzaam in het "Istituto di Fisica" te Genua.

Veel hulp en medewerking heb ik mogen ondervinden van de technische staf van het Kamerlingh Onnes Laboratorium.

Zeer veel steun heb ik ondervonden van de intensieve samenwerking met Dr. H.F.P. K n a a p. De in dit proefschrift beschreven onderzoeken zijn verricht in samenwerking met de heren Drs. H. H u l s m a n, Dr. G. S c o l e s, Dr. W.I. H o n e y w e l l en Dr. T.K. B o s e. Dr. C.J.N. v a n d e n M e i j d e n b e r g was zo welwillend het manuscript te lezen en van kritische commentaar te voorzien.